International Journal of Solids and Structures 47 (2010) 2806–2824

Contents lists available at ScienceDirect

International Journal of Solids and Structures

journal homepage: www.elsevier.com/locate/ijsolstr

An investigation on microscopic and macroscopic stability phenomena of composite solids with periodic microstructure

Domenico Bruno, Fabrizio Greco *, Paolo Lonetti, Paolo Nevone Blasi, Girolamo Sgambitterra

Department of Structural Engineering, University of Calabria, Cosenza, Italy

ARTICLE INFO

Article history:
Received 29 January 2010
Received in revised form 5 May 2010
Available online 19 June 2010

Keywords:
Microscopic stability
Macroscopic stability
Constitutive stability measure
Periodic composite
Finite elements

ABSTRACT

An analysis of the effects of microscopic instabilities on the homogenized response of heterogeneous solids with periodic microstructure and incrementally linear constitutive law is here carried out. In order to investigate the possibility to obtain a conservative prediction of microscopic primary instability in terms of homogenized properties, novel macroscopic constitutive stability measures are introduced, corresponding to the positive definiteness of the homogenized moduli tensors relative to a class of conjugate stress–strain pairs.

Numerical simulations, addressed to hyperelastic microstructural models representing cellular solids and reinforced composites, are worked out through the implementation of an innovative one-way coupled finite element formulation able to determine sequentially the principal equilibrium solution, the incremental equilibrium solutions providing homogenized moduli and the stability eigenvalue problem solution, for a given monotonic macrostrain path. Both uniaxial and equibiaxial loading conditions are considered.

The exact microscopic stability region in the macrostrain space, obtained by taking into account microstructural details, is compared with the macroscopic stability regions determined by means of the introduced macroscopic constitutive measures. These results highlight how the conservativeness of the adopted macroscopic constitutive stability measure with respect to microscopic primary instability, strictly depends on the type of loading condition (tensile or compressive) and the kind of microstructure.

1. Introduction

Heterogeneous solids characterized by a composite microstructure, such as cellular solids, particle and fiber-reinforced materials, are frequently adopted in high performance engineering applications since their microstructure can be designed to optimize their macroscopic properties according to the specific application, thus improving the mechanical properties of single microconstituents and obtaining superior efficiency in comparisons with conventional materials. As a consequence, an accurate prediction of the macroscopic material response of such materials in terms of the microscopic behavior of their constituents, is extremely important. Unfortunately, an accurate analysis of the macroscopic response of heterogeneous materials taking into account a precise description of microstructural details, requires a notable computational cost, since the scale of variation of the constitutive properties, namely the microlength scale, is usually several orders of magnitude smaller than the characteristic dimensions of the structure.

The macroscopic response of heterogeneous materials can be given by using various "homogenization" techniques, which allow to replace the heterogeneous material by an equivalent "homogeneous" material.

In the case of linear elastic solids, after some initial contributions (Hashin and Shtrikman, 1962; Hill, 1965), exact mathematical approaches based on the mathematical procedure of multiscale perturbation and adopting a periodic model for the microstructure, have been proposed (Benssousan et al., 1978; Sanchez-Palencia, 1980; Hassani and Hinton, 1998).

For non-linear heterogeneous solids, the mathematical model must account for non-linear effects related to both the microgeometry and the local constitutive law, since when a classical homogenization procedure is adopted, the macroscopic behavior of microheterogeneous material at finite strains may be often not representative of the microscopic behavior of its constituents due to possible instability phenomena occurring at the microscale. The central difficulty arising in the homogenization of non-linear elastic composites is associated to the non-convexity of the microscopic strain energy density function. As a matter of fact, in the simple case of convex microscopic strain energy functions, as shown in Marcellini, 1978, the homogenization problem can be

* Corresponding author. Address: Department of Structural Engineering, University of Calabria, 87030 Rende, Cosenza, Italy. Tel./fax: +39 984 496916.
E-mail address: f.greco@unical.it (F. Greco).

0020-7683/$ - see front matter © 2010 Elsevier Ltd. All rights reserved.
doi:10.1016/j.ijsolstr.2010.06.013

successfully solved, as in the small strain theory, by minimizing the averaged strain energy density with respect to fluctuation fields periodic over a unit cell, leading to define the representative volume of the microstructure as one periodic cell. On the other hand, the constitutive response of real materials cannot be represented by means of convex energy functions, since convexity is a too strong requirement from the physical point of view (Hill, 1957; Ball, 1977). As a consequence, for general non-convex microscopic strain energy functions, which contrarily to the strictly convex case do not preclude non-uniqueness phenomena on the microscale, by virtue of the notion of Γ-convergence (De Giorgi, 1979), Müller, 1987 defined an homogenized strain energy density function for heterogeneous periodic microstructures corresponding to the minimization of the averaged strain energy density with respect to admissible fluctuation fields that are periodic over an a priori unknown ensemble of periodic cells (possibly infinite). It follows that the extent of the representative volume of the microstructure must be enlarged in such a way to describe the energy minimizing buckling modes, to take into account the possibility that by minimizing the energy over larger domains containing more unit cells, a lower homogenized energy value may be found.

In the study of solids with heterogeneous microstructure, the stability analysis plays a fundamental role, since microscopic failure mechanisms in these materials are often promoted by instability phenomena and owing to the fact that the stability analysis of the microstructured solid establishes the region of validity of the standard homogenization procedure based on unit cell calculations. In particular, the limit of validity for the homogenized models of the heterogeneous solid, can be evaluated only by comparing the onset of the primary instability in the real microstructured solid with the corresponding instability determined by using the homogenized model of the solid.

An accurate stability analysis for composite solids with a generic microstructure must consider both classical buckling type instability modes, dominated by the microstructural geometric configuration and accompanied by a prevalently negative stress state, and constitutive-dominated instabilities arising when tangent moduli of the material reduce greatly attaining eventually negative values and in presence of a positive stress state (Greco and Luciano, 2005). A typical example of the former kind of instability is fiber microbuckling in laminated microstructures loaded primarily in compression (Triantafyllidis and Maker, 1985; Miehe et al., 2002), whereas the latter kind of instability may occur in cellular and particle-reinforced microstructures when loaded prevalently in tension (Michel et al., 2007, for example).

In order to avoid an excessive computational effort, usually the stability analysis of elastic composite solids with periodic microstructure is performed by using their macroscopic properties. Unfortunately, when the stability analysis is based on the homogenized constitutive properties, microscopic instability mechanisms cannot be accurately predicted and a direct analysis of the heterogeneous solid, including a detailed description of the microstructure, becomes necessary to determine the exact microstructural instability mechanisms. On the other hand, several complications arise in a direct stability analysis since finite changes in geometry and in constitutive properties must be taken into account and owing to the irregularity of the geometry of the microstructure. It follows that, an accurate analysis of the interrelations between instabilities occurring on the macro- and microscales becomes fundamental to investigate the effectiveness of a stability investigation based on the homogenized composite properties.

Several analyses on the effective properties of non-linear elastic composites with periodic microstructure including investigations on instability phenomena, have been carried out in the literature. For instance, with reference to elastomeric composites containing periodic holes, it was pointed out that at sufficiently large macroscopic strains the homogenized incremental moduli tensor can lose its strong ellipticity even if the microscopic tangential moduli tensor satisfy the strongly ellipticity condition (Abeyaratne and Triantafyllidis, 1984). Moreover, with reference to a two-dimensional layered medium under axial loading characterized by a rate independent constitutive law, a strict connection between structural bifurcation at the microscopic scale and loss of strong ellipticity condition for the macroscopic incremental moduli tensor was established, by noting that when bifurcation occurs at a wavelength much larger than the unit cell size then it corresponds to the loss of strong ellipticity condition for the homogenized incremental moduli tensor (Triantafyllidis and Maker, 1985). By using the results of Müller, 1987, then Geymonat et al., 1993 proved the connection between microscopic bifurcation and loss of macroscopic strict rank-one convexity in the framework of functional analysis, for arbitrary solids with periodic microstructures. In this work, it was also proved that if the wavelength of the bifurcation primary eigenmode is much larger compared to the unit cell size, the onset of the corresponding instability of the periodic principal solution can be detected as a loss of ellipticity of the corresponding one-cell homogenized tangent moduli of the solid.

A comprehensive treatment of the transition from micro- to macrovariables of a representative volume element (RVE) of a finitely deformed composite has been explored, starting from the pioneering work of Hill, 1972, in Nemat-Nasser, 1999.

Numerical homogenization techniques based on finite element formulations in the large strain context have been recently developed, for example, in Miehe et al., 2002 for elastic composites, where a numerical investigation of the interaction between microscopic and macroscopic instability phenomena has been also carried out, and by Miehe, 2003 for inelastic composites by assuming that the overall properties of the microstructure can be obtained by the minimization of a suitably defined averaged strain energy. Accurate numerical determinations of the region of microscopic stability and of the region of macroscopic stability, intended as the region where the strong ellipticity condition for the homogenized moduli tensor still holds, have been carried out for specific microstructural models in Triantafyllidis and Bardenhagen, 1996, Nestorović' and Triantafyllidis, 2004, Triantafyllidis et al., 2006, and Michel et al., 2007. The instability of fiber-reinforced elastomers has been also studied in Lopez-Pamies and Ponte Castañeda, 2006a,Lopez-Pamies and Ponte Castañeda, 2006b,Lopez-Pamies and Ponte Castañeda, 2009 by using the second-order tangent homogenization method (Ponte Castañeda and Tiberio, 2000). Experimental and analytical studies on the failure of fiber-reinforced polymer matrix composites have been developed in a two-dimensional context by Kyriakides et al., 1995. These studies have been extended in Hsu et al., 1998, by modeling the composite as a three-dimensional solid, and in Vogler et al., 2000, by considering combined axial compression and shear loading. Fiber microbuckling has been analyzed by adopting computational homogenization approaches in Grandidier et al., 1992, Lee and Waas, 1999, and Drapier et al., 2001 to describe the compressive failure of long-fiber composites.

In addition, conditions for microscopic symmetric bifurcations in cellular solids have been developed by Ohno et al., 2002, in the context of the homogenization theory in presence of finite strains and by using an updated Lagrangian formulation. Moreover, a numerical methodology able to solve non-linear homogenization problems, including microscopic and macroscopic instabilities, and based on a multilevel finite element approach, has been proposed in Nezamabadi et al., 2009. Finally, the efficacy of homogenization techniques for microstructured materials of cellular type subjected to large deformations has been analyzed in Cricri and Luciano, 2003, by comparisons between micro- and macroinstability mechanisms and adopting the Biot strain measure to define a macrofailure surface.

The above literature review highlights that a fundamental measure of macroscopic stability, based on homogenized constitutive properties, for a heterogeneous solid with periodic microstructure is that based on the strong ellipticity condition of the homogenized moduli tensor. As a matter of fact, the strong ellipticity of the homogenized solid incremental moduli or, equivalently, the strict local rank-one convexity of the homogenized strain energy function, ensures infinitesimal stability under Dirichlet boundary conditions when the macroscopic incremental moduli tensor is spatially constant and excludes solutions with discontinuous deformation gradients (shear bands) in the homogenized material. The strong ellipticity condition is able to exactly predict the onset of microscopic instability of the periodic principal solution along a monotonic loading process when the microscopic instability mode is global in nature, i.e. its wavelength is much larger in comparison with the unit cell size (this circumstance may occur, for instance, in composite materials reinforced with relatively thick fibers or in particle-reinforced materials, loaded prevalently in compression). On the contrary, an unconservative estimation of the primary microscopic instability load is obtained by the above mentioned macroscopic stability measure, in the more general case when the instability mode is local in nature, namely its wavelength is comparable to the unit cell size, since the homogenized moduli tensor remains strongly elliptic at the onset of the primary microscopic instability. The latter kind of instabilities may occur, for instance, in cellular solids or in fiber-reinforced materials with relatively thin fibers (fiber-buckling).

In this work, a stability analysis on the micro- and macroscales is carried out, both from a theoretical and numerical point of views, in order to investigate alternative macroscopic conditions able to provide accurate prediction of the microscopic instability mechanisms in composite solids with periodic microstructure. Firstly, with reference to incrementally linear constitutive laws, theoretical details about the homogenization problem and the stability conditions related to the micro- to macrotransition, for a heterogeneous solid with periodic microstructure undergoing deformations at finite strains, are provided. Then alternative macroscopic constitutive stability measures are defined, corresponding to the positive definiteness of homogenized moduli tensors associated with a class of work conjugate stress–strain measures, and their ability to obtain conservative prediction of the primary instability load of the microstructure is investigated. After the description of the numerical method proposed to compute the homogenized tangent moduli, the microscopic and macroscopic primary instability loads and the corresponding eigenmodes, numerical applications devoted to cellular and particle-reinforced composite microstructures with hyperelastic constituents of neo-Hookean or Gent types, are provided. Finally, the results of calculations, given in terms of microscopic and macroscopic stability predictions for different loading paths, are followed by the conclusions where these results are commented.

2. Theoretical formulation

In this section, the stability problem of a perfectly periodic incrementally linear composite solid is formulated. The main objective is to define the critical load level corresponding to the first loss of stability along a prescribed loading path, and to discuss the stability estimates which can be obtained by means of the homogenized composite properties. The section is divided into five parts. In the first four parts the main equations of the homogenization procedure necessary for a better understanding of the subsequent developments are summarized, and the basic notation used in the paper is defined. Specifically, the macroscopic properties of a periodic microstructure are formulated in Sections 2.1 and 2.2 and the microscopic stability problem, which requires the examination of all perturbations of the equilibrium fluctuation field periodic over a unit cell, is introduced in Section 2.3. Then the classical macroscopic stability criterion based on the strong ellipticity condition of the homogenized moduli tensor is also recalled in Section 2.4. Results shown in Sections 2.1–2.4 can be considered essentially as review of the existing literature.

In the last part, the concept of macroscopic constitutive stability measures is presented as a way to investigate the microscopic stability problem in terms of the homogenized properties of the periodic heterogeneous solid based on calculations simply performed on a unit cell. Novel macroscopic constitutive stability measures are defined by means of constitutive inequalities involving the homogenized tangent moduli tensor associated to a sub-class of work conjugate stress–strain measures. This is a central aspect of this work which makes the paper innovative, since to the authors' knowledge there are no similar macroscopic constitutive criteria available in the literature. The above mentioned macroscopic constitutive stability measures are also derived in an original way by means a correct multi-scale stability analysis.

2.1. Homogenization methodology: microscopic and macroscopic variables

Consider an heterogeneous solid whose periodic microstructure is characterized by a unit cell occupying the domain V_i in the stress-free undeformed configuration. The unit cell generates by periodic repetition the whole microstructure, which is assumed to be associated with an infinitesimal neighborhood of a generic material point $\overline{\boldsymbol{X}}$ of the corresponding homogenized continuum, which in its initial undeformed configuration occupies the region $\overline{V}_{(i)}$ (see Fig. 1).

It is assumed that the scale at which the microstructure is defined (microscopic scale, l_{micro}) is small enough for the heterogeneities to be identified, while the homogenized continuum is defined at a macroscopic scale, l_{macro}, so large that the heterogeneities can be 'smeared-out'. The initial and current position vectors of a material point of the microstructure are denoted by $\boldsymbol{X}$ and $\boldsymbol{x}$. The nonlinear deformation of the microstructure, defined by $\boldsymbol{x}(\boldsymbol{X})$: $V_{(i)} \to V$, maps points $\boldsymbol{X}$ of the initial configuration $V_{(i)}$ onto points $\boldsymbol{x}$ of the actual configuration V of the microstructure. The deformation gradient at $\boldsymbol{X}$ is denoted as $\boldsymbol{F}(\boldsymbol{X})$, where $\boldsymbol{F} = \partial \boldsymbol{x}(\boldsymbol{X})/\partial \boldsymbol{X}$, and the displacement field at $\boldsymbol{X}$ is denoted by $\boldsymbol{u}(\boldsymbol{X})$, where $\boldsymbol{u} = \boldsymbol{x}(\boldsymbol{X}) - \boldsymbol{X}$.

According to a rate independent material model, the incremental constitutive law, governing the response at a microscopic point $\boldsymbol{X}$, is assumed linear:

$$\dot{\boldsymbol{T}}_R = \boldsymbol{C}^R(\boldsymbol{X}, \boldsymbol{F})[\dot{\boldsymbol{F}}], \tag{1}$$

where $\dot{\boldsymbol{T}}_R$ is the rate of the first Piola–Kirchhoff stress tensor, $\dot{\boldsymbol{F}}$ is the deformation gradient rate and $\boldsymbol{C}^R$ is the corresponding fourth-order tensor of nominal moduli, a $V_{(i)}$-periodic function of $\boldsymbol{X}$. The rate of a field quantity is defined as its derivative with respect to a time-like parameter which increases monotonically with the evolution of the loading process, since only quasi-static loading conditions are considered here. It is further assumed that the nominal moduli tensor satisfies the major symmetry condition, namely $C^R_{ijkl} = C^R_{klij}$. Eq. (1) is able to model a wide range of materials, such as elastic or hypoelastic materials. Specifically, when the microscopic constitutive behavior is hyperelastic, the nominal moduli tensor and the nominal stress tensor can be defined as:

$$\boldsymbol{C}^R(\boldsymbol{X}, \boldsymbol{F}) = \frac{\partial^2 W(\boldsymbol{X}, \boldsymbol{F})}{\partial \boldsymbol{F} \partial \boldsymbol{F}}, \quad \boldsymbol{T}_R = \frac{\partial W(\boldsymbol{X}, \boldsymbol{F})}{\partial \boldsymbol{F}},$$

where W is the strain energy density function that is a non-convex function of the deformation gradient $\boldsymbol{F}$, $\partial^2 W(\boldsymbol{X},\boldsymbol{F})/\partial \boldsymbol{F} \partial \boldsymbol{F}$ denotes a

fourth-order tensor whose components are $C^R_{ijkl} = \partial^2 W(\boldsymbol{X},\boldsymbol{F})/\partial F_{ij}\partial F_{hk}$ and $\partial W(\boldsymbol{X},\boldsymbol{F})/\partial \boldsymbol{F}$ a second-order tensor whose components are $T^R_{ij} = \partial W(\boldsymbol{X},\boldsymbol{F})/\partial F_{ij}$.

Coherently with the classical assumption of the homogenization theory, the macroscopic constitutive response of the microstructure is based on an equilibrium state neglecting volume forces, implying that the local stress field $\boldsymbol{T}_R$ is divergence-free, namely $\mathrm{Div}(\boldsymbol{T}_R) = 0$ in $V_{(i)}$.

The macroscopic first Piola–Kirchhoff stress and the macroscopic deformation gradient tensors are defined in terms of boundary data of the traction field $\boldsymbol{t}_R$ and the deformation field $\boldsymbol{x}(\boldsymbol{X})$ according to (Hill, 1972), respectively, as:

$$\overline{\boldsymbol{T}}_R = \frac{1}{|V_{(i)}|}\int_{\partial V_{(i)}} \boldsymbol{t}_R(\boldsymbol{X}) \otimes \boldsymbol{X} ds_{(i)}, \quad \overline{\boldsymbol{F}} = \frac{1}{|V_{(i)}|}\int_{\partial V_{(i)}} \boldsymbol{x}(\boldsymbol{X}) \otimes \boldsymbol{n}_{(i)} ds_{(i)}, \tag{2}$$

where $\otimes$ is the tensor product and $\boldsymbol{n}_{(i)}$ denotes the outward normal at $\boldsymbol{X} \in \partial V_{(i)}$.

The microscopic deformation can be expressed as the following function of the macrodeformation gradient $\overline{\boldsymbol{F}}$:

$$\boldsymbol{x}(\boldsymbol{X}) = \overline{\boldsymbol{F}}\boldsymbol{X} + \boldsymbol{w}(\boldsymbol{X}), \tag{3}$$

where the linear part $\overline{\boldsymbol{F}}\boldsymbol{X}$ represents a homogeneous deformation, and the correction part $\boldsymbol{w}(\boldsymbol{x})$, usually referred to as the fluctuation field, is associated to a non-homogeneous deformation. As a consequence the microscopic deformation gradient assumes the following expression:

$$\boldsymbol{F}(\boldsymbol{X}) = \overline{\boldsymbol{F}} + \nabla \boldsymbol{w}(\boldsymbol{X}). \tag{4}$$

It is worth noting that Eqs. (2) defines a coupling between the macroscopic deformation of the macrocontinuum, characterized by the macrodeformation gradient $\overline{\boldsymbol{F}}$ in the neighborhood of a typical point $\overline{\boldsymbol{X}}$, and the deformation of the microstructure.

Eq. $(2)_1$ leads to the following constraint in terms of the fluctuation field:

$$\int_{\partial V_{(i)}} \boldsymbol{w} \otimes \boldsymbol{n}_{(i)} ds_{(i)} = 0. \tag{5}$$

which can be satisfied for periodic fluctuation fields on the unit cell boundary:

$$\boldsymbol{w}(\boldsymbol{X}^+) = \boldsymbol{w}(\boldsymbol{X}^-) \text{ on } \partial V_{(i)}. \tag{6}$$

As illustrated in Fig. 2, the periodicity of the field $\boldsymbol{w}(\boldsymbol{X})$ implies that all components of $\boldsymbol{w}(\boldsymbol{X})$ assume identical values at points on opposite sides of the boundary $\partial V_{(i)}$, $\partial V^+_{(i)}$ and $\partial V^-_{(i)}$, with outwards normals $\boldsymbol{n}^+_{(i)} = -\boldsymbol{n}^-_{(i)}$ at two associated points $\boldsymbol{X}^+ \in \partial V^+_{(i)}$ and $\boldsymbol{X}^- \in \partial V^-_{(i)}$, which are deduced by translation parallel to the directions of the periodicity vectors spanning $V_{(i)}$. By virtue of the assumed $V_{(i)}$-periodic distribution of material and geometrical properties of the heterogeneous solid with respect to a unit cell, the local boundary conditions equation (6) suffice to completely determine its mechanical response and guarantee a periodic distribution of the stress and strain field quantities. However, the mechanical response of the heterogeneous solid at a given macrodeformation gradient, can be determined by means of computations performed over one unit cell only when the equilibrium solution of the microstructure is stable, otherwise an assembly of unit cells must be considered. This aspect will be clarified in the following section.

2.2. Calculation of the macroscopic response

According to the incremental character of the constitutive law, attention is now focused on the incremental homogenized response of the solid. Suppose that the microstructure at a generic stage of a quasi-static loading path $\overline{\boldsymbol{F}}(\beta)$ (with the load parameter $\beta \geqslant 0$ increasing monotonically with increasing macroscopic load) beginning from the initial configuration associated to the region $V_{(i)}$ (i.e. with $\overline{\boldsymbol{F}}(\beta) = 1$ when $\beta = 0$) occupies the region V defined by the deformation:

$$\boldsymbol{x}(\boldsymbol{X}) = \overline{\boldsymbol{F}}(\beta)\boldsymbol{X} + \boldsymbol{w}_{\overline{\boldsymbol{F}}(\beta)}(\boldsymbol{X}),$$

and driven by the macroscopic load $\overline{\boldsymbol{F}}(\beta)$. The deformed configuration in which the microstructure occupies the region V, is assumed to be known. The associated equilibrium solution is defined in term of the fluctuation solution $\boldsymbol{w}_{\overline{\boldsymbol{F}}}(\boldsymbol{X})$ at the given macrodeformation gradient of the following unit-cell deformation variational problem:

$$\int_{V_{(i)}} \boldsymbol{T}_R(\boldsymbol{X}, \overline{\boldsymbol{F}} + \nabla \boldsymbol{w}_{\overline{\boldsymbol{F}}}) \cdot \nabla \delta \boldsymbol{w} dV_{(i)} = 0 \quad \forall \delta \boldsymbol{w} \in H^{1,p}(V_{(i)\#}), \tag{7}$$

where $H^{1,p}(V_{(i)\#})$ denotes the usual Sobolev space of vector valued functions periodic over the unit cell $V_{(i)} = [0,1]^N$, and the abbreviated notation # appended to a region denotes the periodic properties of a field on the boundary of the region. Analogously, the antiperiodicity of a field quantity, implying that the field quantity takes opposite values at points on opposite sides of the boundary $\partial V_{(i)}$ of the unit cell, will be denoted by $-\#$.

The variational equation (7) is consistent with an equilibrium state of the microstructure with anti-periodic tractions on the external surface $\partial V_{(i)}$ of the microstructure and zero tractions on the boundary $\partial H_{(i)}$ of the holes, as confirmed by the associated Euler–Lagrange equations:

$$\begin{cases} Div \boldsymbol{T}_R = 0 \text{ in } V_{(i)} \\ (\boldsymbol{T}_R \boldsymbol{n}_{(i)})^+ = -(\boldsymbol{T}_R \boldsymbol{n}_{(i)})^- \text{ on } \partial V_{(i)}, \\ \boldsymbol{T}_R \boldsymbol{n}_{(i)} = 0 \text{ on } \partial H_{(i)} \end{cases} \tag{8}$$

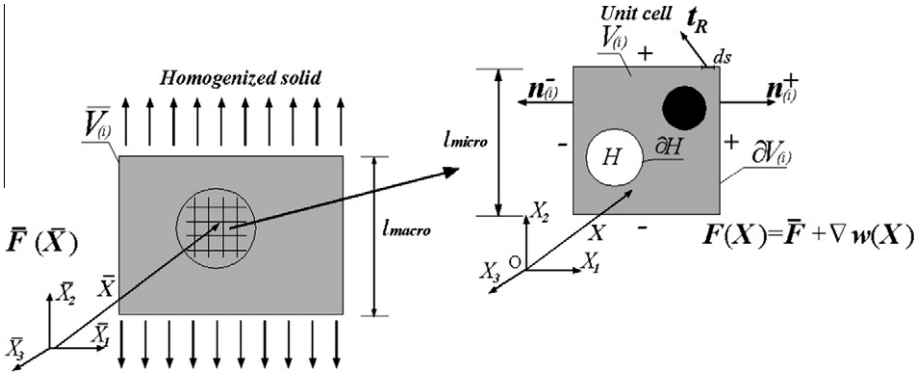

Fig. 1. Representation of the homogenized solid and of the unit cell defining the periodic microstructure attached to a generic material point $\overline{X}$.

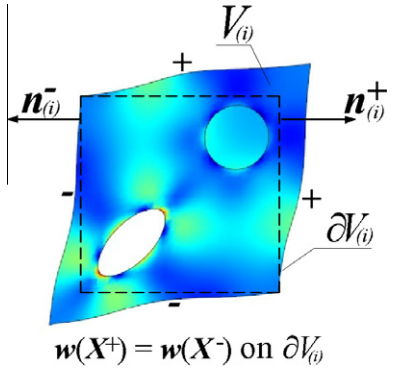

Fig. 2. Deformed unit cell satisfying the periodic boundary constraints for the fluctuation field.

where $(\,)^{+}$ and $(\,)^{-}$ denote variables evaluated at two associated points $\boldsymbol{X}^{+} \in \partial V^{+}$ and $\boldsymbol{X}^{-} \in \partial V^{-}$, respectively, whereas $\partial H_{(i)}$ denotes the boundary of the eventual hole part of the unit cell. The equilibrium solution is determined by Eq. (8) up to a possible rigid body motions which must be excluded by imposing artificial constraints.

The sequence of equilibrium solutions for the unit-cell deformation problem generated by the macroscopic loading path $\overline{\boldsymbol{F}}(\beta)$, is referred to as the "principal solution path", assuming a unique solution for each value of the loading parameter β.

Consider the incremental equilibrium problem induced at the microscopic scale by an incremental change in the macroscopic deformation gradient $\dot{\overline{\boldsymbol{F}}}(\beta)$. Once the microscopic distribution of the nominal moduli tensor $\boldsymbol{C}^{R}(\boldsymbol{X}, \overline{\boldsymbol{F}} + \nabla \boldsymbol{w}_{\overline{\boldsymbol{F}}})$ is determined by virtue of Eq. (7), the following local problem can be solved:

$$\int_{V_{(i)}} \boldsymbol{C}^{R}(\boldsymbol{X}, \overline{\boldsymbol{F}}) \left[\dot{\overline{\boldsymbol{F}}} + \nabla \dot{\boldsymbol{w}}_{\dot{\overline{\boldsymbol{F}}}}\right] \cdot \nabla \delta \dot{\boldsymbol{w}} dV_{(i)} = 0 \quad \forall \delta \dot{\boldsymbol{w}} \in H^{1,p}(V_{(i)\#}). \tag{9}$$

In Eq. (9) $\dot{\boldsymbol{w}}_{\dot{\overline{\boldsymbol{F}}}}$ denotes the incremental fluctuation field induced by $\dot{\overline{\boldsymbol{F}}}(\beta)$ and determines the microstructure incremental equilibrium solution with antiperiodic incremental tractions $\dot{\boldsymbol{t}}_{R} \in V_{(i)-\#}$, i.e.. $\dot{\boldsymbol{t}}_{R}(\boldsymbol{X}^{+}) = -\dot{\boldsymbol{t}}_{R}(\boldsymbol{X}^{-})$ on $\partial V_{(i)}$, vanishing tractions $\dot{\boldsymbol{t}}_{R}(\boldsymbol{X}) = \boldsymbol{0}$ on the boundary $\partial H_{(i)}$ of eventual hole parts, and periodic boundary constraints, $\dot{\boldsymbol{w}}(\boldsymbol{X}) \in V_{(i)\#}$. Incremental rigid body displacements of the unit cell, included in the solution to Eq. (9), must be excluded by introducing appropriate constraints.

The fundamental identity $\dot{\overline{\boldsymbol{T}}}_{R} = \dot{\overline{\boldsymbol{T}}}_{R}$, (Nemat-Nasser, 1999), stating that the increment of the macroscopic stress tensor is equal to the macroscopic incremental stress tensor, in conjunction with the following definition macroscopic constitutive response in terms of the homogenized tangent moduli tensor $\overline{\boldsymbol{C}}^{R}(\overline{\boldsymbol{F}})$:

$$\dot{\overline{\boldsymbol{T}}}_{R} = \overline{\boldsymbol{C}}^{R}(\overline{\boldsymbol{F}})[\dot{\overline{\boldsymbol{F}}}], \tag{10}$$

leads to determine the homogenized tangent modulus tensor of the solid as:

$$\overline{\boldsymbol{C}}^{R}(\overline{\boldsymbol{F}})[\dot{\overline{\boldsymbol{F}}}] = \frac{1}{|V_{(i)}|} \int_{V_{(i)}} \boldsymbol{C}^{R}(\boldsymbol{X}, \overline{\boldsymbol{F}})[\dot{\overline{\boldsymbol{F}}} + \nabla \dot{\boldsymbol{w}}_{\dot{\overline{\boldsymbol{F}}}}] dV_{(i)}. \tag{11}$$

As shown in Eq. (11), the computation of homogenized moduli tensor requires the knowledge of the local incremental problem solution $\dot{\boldsymbol{w}}_{\dot{\overline{\boldsymbol{F}}}}$. In view of numerical applications, it is convenient to obtain from Eq. (11) the components of the homogenized moduli tensor as:

$$\overline{C}^{R}_{ijhk}(\overline{\boldsymbol{F}}) = \frac{1}{|V_{(i)}|} \int_{V_{(i)}} C^{R}_{ijmn}(\boldsymbol{X}, \overline{\boldsymbol{F}}) \left[I^{hk}_{mn} + \nabla \dot{w}_{hk}\right] dV_{(i)}, \tag{12}$$

in terms of the incremental fluctuation field $\dot{\boldsymbol{w}}_{hk}$ induced by unit value components of the macroscopic deformation increment $\dot{\overline{\boldsymbol{F}}} = \boldsymbol{I}^{hk}$, where $I^{hk}_{mn} = \delta_{mh}\delta_{nk}$.

As already noted in Geymonat et al., 1993, the homogenized moduli tensor can be equivalently defined by:

$$\overline{\boldsymbol{C}}^{R}(\overline{\boldsymbol{F}})[\dot{\overline{\boldsymbol{F}}}] \cdot \dot{\overline{\boldsymbol{F}}} = \min_{\dot{\boldsymbol{w}} \in H^{1,p}(V_{(i)}\#)} \frac{1}{|V_{(i)}|} \int_{V_{(i)}} \boldsymbol{C}^{R}(\boldsymbol{X}, \overline{\boldsymbol{F}})[\dot{\overline{\boldsymbol{F}}} + \nabla \dot{\boldsymbol{w}}_{\dot{\overline{\boldsymbol{F}}}}] \cdot \left(\dot{\overline{\boldsymbol{F}}} + \nabla \dot{\boldsymbol{w}}_{\dot{\overline{\boldsymbol{F}}}}\right) dV_{(i)} \tag{13}$$

and consequently its components can be computed as:

$$\overline{C}^{R}_{ijhk}(\overline{\boldsymbol{F}}) = \frac{1}{|V_{(i)}|} \int_{V_{(i)}} C^{R}_{pqmn}(\boldsymbol{X}, \overline{\boldsymbol{F}})[I^{hk}_{mn} + \nabla \dot{w}_{hk}] \cdot [I^{ij}_{pq} + \nabla \dot{w}_{ij}] dV_{(i)}, \tag{14}$$

which can be obtained by taking the second partial derivative of the expression (13) with respect to the macroscopic deformation gradient increment, i.e. $\overline{C}^{R}_{ijhk}(\overline{\boldsymbol{F}}) = \partial^{2}\overline{\boldsymbol{C}}^{R}(\overline{\boldsymbol{F}})[\dot{\overline{\boldsymbol{F}}}] \cdot \dot{\overline{\boldsymbol{F}}} / \partial \dot{\overline{F}}_{ij} \partial \dot{\overline{F}}_{hk}$. It follows that $\dot{\boldsymbol{w}}_{hk}$ coincides with the derivatives of the equilibrium fluctuation increment functions $\dot{\boldsymbol{w}}_{\dot{\overline{\boldsymbol{F}}}}$, namely $\dot{\boldsymbol{w}}_{hk} = \partial \dot{\boldsymbol{w}}_{\dot{\overline{\boldsymbol{F}}}} / \partial \dot{\overline{\boldsymbol{F}}}_{hk}$.

The above definition of the homogenized moduli tensor based on computations over one unit cell, is valid only when the equilibrium configuration of the microstructure is incrementally stable, otherwise the homogenization procedure must be performed over a larger assembly of unit cells (possibly infinite).

When the microscopic constituents are hyperelastic, the homogenized strain energy function $\overline{W}(\overline{\boldsymbol{F}})$ can be determined as the minimum volume average of the microscopic strain energy function with respect to admissible fluctuation fields $\boldsymbol{w}(\boldsymbol{X})$, belonging to the Sobolev space of vector valued functions periodic over all possible ensemble of $k^{N} = [0,k]^{N}$ unit cells ($N = 2$ or 3 for two- or three-dimensional problems, respectively), $H^{1,p}(k^{N}V_{(i)}\#)$, with k an arbitrary integer (Müller, 1987):

$$\overline{W}(\overline{\boldsymbol{F}}) = \inf_{k \in \mathbb{N}} \left\{ \min_{\boldsymbol{w} \in H^{1,p}(k^{N}V_{i}\#)} \left\{ \frac{1}{k^{N}|V_{(i)}|} \int_{k^{N}V_{(i)}} W(\boldsymbol{X}, \overline{\boldsymbol{F}} + \nabla \boldsymbol{w}) dV_{(i)} \right\} \right\}. \tag{15}$$

The strain energy function W is assumed to be objective, i.e. $W(\boldsymbol{Q}\boldsymbol{F}) = W(\boldsymbol{F})$ for all proper orthogonal $\boldsymbol{Q}$ and arbitrary deformation gradients $\boldsymbol{F}$. It follows that also the homogenized strain energy function, is unaffected by a superposed macroscopic rigid body motion after deformation.

As can be verified by a formal calculation of the first and second derivatives of the homogenized strain energy function based on Eq. (15), which makes use of Eq. (7), the macrostress potential and homogenized moduli tensor are defined in terms of the first and second derivatives of the macrostress potential with respect to the macrodeformation gradient:

$$\overline{\boldsymbol{T}}_{R} = \frac{\partial \overline{W}}{\partial \overline{\boldsymbol{F}}}, \quad \overline{\boldsymbol{C}}^{R} = \frac{\partial^{2}\overline{W}}{\partial \overline{\boldsymbol{F}} \partial \overline{\boldsymbol{F}}}. \tag{16}$$

When the microscopic strain energy function $W(\boldsymbol{F})$ is a convex function of $\boldsymbol{F}$, it turns out that the macroscopic energy function coincides with the one-cell homogenized strain energy function, defined by the following minimization problem:

$$\overline{W}^{1}(\overline{\boldsymbol{F}}) = \min_{\boldsymbol{w} \in H^{1,p}(V_{i}\#)} \left\{ \frac{1}{|V_{(i)}|} \int_{V_{(i)}} W(\boldsymbol{X}, \overline{\boldsymbol{F}} + \nabla \boldsymbol{w}) dV_{(i)} \right\}. \tag{17}$$

The minimization principles (15) and (17) are consistent with an equilibrium state of the hyperelastic microstructure governed by Eq. (8) written with reference to an assembly of unit cells or to a unit cell, respectively.

It is worth noting that realistic materials must be modeled by using a non-convex strain energy functions. As a matter of fact, convexity requirement is usually a too strong and physically unacceptable restriction (Hill, 1957; Ball, 1977). For instance, the strict variant of the convexity condition implies uniqueness of solutions

for the fluctuation field, thus precluding microscopic buckling of the heterogeneous microstructure.

On the other hand non-convex microenergy functions are able to take into account non-uniqueness phenomena such as buckling on the microscale. These phenomena are of notable importance since may lead to obtain lower values for the homogenized strain energy function, by minimization over domains containing several unit cells. In this situation, Eq. (15) determines the current fluctuation field and defines the size of the representative volume of the microstructure, which is a priori unknown, also capturing the minimizing microbuckling mode.

From Eq. (15) it results that $\overline{W}(\overline{\boldsymbol{F}}) \leqslant \overline{W}^1(\overline{\boldsymbol{F}})$ and that the equality holds only when the minimizing fluctuation field based on the unit cell computation is also the minimizing fluctuation field for any possible unit cell assembly. The application of Eq. (15) involves notable difficulties associated to the infinity of the required domain and implies a full space investigation on the microscale. As a consequence it is preferable to take advantage of Eq. (17), involving a much simpler calculation, although this equation gives the correct results only in the region of the macroscopic strain space where $\overline{W}(\overline{\boldsymbol{F}}) = \overline{W}^1(\overline{\boldsymbol{F}})$, namely the region of validity of the one-cell homogenization. The region of validity of the one-cell homogenization, useful to justify the use of Eq. (17), can be determined by means of a microscopic stability analysis, as will be shown in the following section.

2.3. Microscopic stability analysis

The current equilibrium configuration $k^N V$, individuated by the macroscopic strain $\overline{\boldsymbol{F}}$ and the corresponding fluctuation solution $\boldsymbol{w}_{\overline{\boldsymbol{F}}}$, is now taken as reference to determine the response of the microstructure to superimposed infinitesimal deformations. To this aim an additional microscopic displacement field $\boldsymbol{u}(\boldsymbol{x},\tau)$ from the reference configuration is considered, compatible with the essential boundary conditions on the boundary of $k^N V$. This implies $\boldsymbol{u}(\boldsymbol{x},\tau=0)=0$ on $\partial k^N V$ and $\boldsymbol{u}(\boldsymbol{x}^+,\tau)=\boldsymbol{u}(\boldsymbol{x}^-,\tau)$ on $\partial k^N V$, where τ is a time-like parameter with $\tau \geqslant 0$. The microscopic displacement field $\boldsymbol{u}$ deforms the microstructure from the reference configuration $k^N V$ to the generic configuration $k^N V(\tau)$, as sketched in Fig. 3. The gradient of the microscopic deformation field relative to the reference configuration V, is denoted by $\boldsymbol{F}_{(0)}(\boldsymbol{x},\tau)$.

The displacement field and the gradient of the additional deformation can be expressed as a series expansion of the time-like parameter τ:

$$\boldsymbol{u}(\boldsymbol{x},\tau) = \dot{\boldsymbol{u}}_0(\boldsymbol{x})\tau + \boldsymbol{o}(\tau), \quad \boldsymbol{F}_{(0)}(\boldsymbol{x},\tau) = \boldsymbol{I} + \boldsymbol{L}(\boldsymbol{x})\tau + \boldsymbol{O}(\tau). \tag{18}$$

For small values of τ he additional displacement field represents an infinitesimal deformation (also called incremental) from the current configuration $k^N V$ and the displacement rate field $\dot{\boldsymbol{u}}(\boldsymbol{x})$ can be considered as the "quasi-static" velocity field, whereas the gradient $\boldsymbol{L}(\boldsymbol{x})$ is the velocity gradient. Eq. (3) leads to:

$$\begin{aligned}\boldsymbol{u}(\boldsymbol{x},\tau) &= \dot{\boldsymbol{u}}_0(\boldsymbol{x})\tau + \boldsymbol{o}(\tau) = \left(\dot{\overline{\boldsymbol{F}}}_{(0)}\boldsymbol{x} + \dot{\boldsymbol{w}}(\boldsymbol{x})\right)\tau + \boldsymbol{o}(\tau)\\ &= \dot{\boldsymbol{w}}(\boldsymbol{x})\tau + \boldsymbol{o}(\tau),\end{aligned} \tag{19}$$

where $\dot{\overline{\boldsymbol{F}}}_{(0)}$ is the rate of the macroscopic deformation gradient relative to configuration $k^N V$, evaluated in the current configuration, which vanishes due to the assumed periodicity of the additional displacement field, and $\dot{\boldsymbol{w}}(\boldsymbol{x})$ is the fluctuation field velocity. It turns out that $\boldsymbol{L} = \nabla\dot{\boldsymbol{w}}(\boldsymbol{x}) = \partial\dot{\boldsymbol{w}}(\boldsymbol{x})/\partial\boldsymbol{x}$.

According to the incremental description of material response, the incremental version of the classical criterion of stability of the current equilibrium configuration (Hill, 1978), is here used with the current configuration $k^N V$ taken as the reference one. Taking the second-order series expansion of the internal deformation work D:

$$\begin{aligned}D &= \int_0^t \int_{k^N V} [\boldsymbol{T}_{R(0)}(\boldsymbol{x},\tau)\cdot\dot{\boldsymbol{F}}_{(0)}(\tau)]dVd\tau\\ &= \left\{\int_{k^N V}[\boldsymbol{T}_{R(0)}(\boldsymbol{x},\tau)\cdot\dot{\boldsymbol{F}}_{(0)}(\tau)]_{\tau=0}dV\right\}t\\ &\quad + \left\{\int_{k^N V}[\boldsymbol{T}_{R(0)}(\boldsymbol{x},\tau)\cdot\dot{\boldsymbol{F}}_{(0)}(\tau)]_{\tau=0}dV\right\}\frac{t^2}{2} + o(t^2)\end{aligned}$$

and of the work done by the antiperiodic tractions $\boldsymbol{t}_{R(0)}$ acting in the examined equilibrium configuration

$$L = \int_0^t \left[\int_{\partial k^N V} \boldsymbol{t}_{R(0)}\cdot\dot{\boldsymbol{u}}ds\right]d\tau = \int_{\partial k^N V}\boldsymbol{T}_0\boldsymbol{n}\cdot\left(\dot{\boldsymbol{u}}_0 t + \ddot{\boldsymbol{u}}_0\frac{t^2}{2}\right)ds + o(t^2)$$

during the additional deformation from $k^N V$ to $k^N V(\tau)$, leads to:

$$D - L = \left(\int_{k^N V}\dot{\boldsymbol{T}}_{R(0)}\cdot\boldsymbol{L}dV\right)\frac{t^2}{2} + o(t^2), \tag{20}$$

where $\boldsymbol{T}_{R(0)}$ is the first Piola–Kirchhoff stress tensor based on the configuration $k^N V(\tau=0)$ and $\boldsymbol{T}_0$ is the Cauchy stress tensor in the reference configuration $k^N V$ which corresponds to $\boldsymbol{T}_{R(0)}(\boldsymbol{x},\tau=0)$. The first-order terms vanish due to equilibrium in the examined configuration $k^N V$ and dead loading is assumed on $\partial k^N V$, namely $\boldsymbol{t}_{R(0)}$ is independent on τ.

In the above equations dV and ds denote the reference volume and area elements, respectively. Moreover, due to the assumed periodicity for displacement field and antiperiodicity of surface tractions, L is identically zero.

The structural stability condition of the microstructure at the macroscopic deformation $\overline{\boldsymbol{F}}$ is based on the positive definiteness of the functional represented in Eq. (20), referred to as the stability functional, for every incremental deformations satisfying the essential periodic boundary constraints. Writing the incremental constitutive law, with the reference configuration coinciding with the current one, leads to:

$$\dot{\boldsymbol{T}}_{R(0)} = \boldsymbol{C}_0^{\boldsymbol{R}}(\boldsymbol{F})[\boldsymbol{L}], \tag{21}$$

where $\boldsymbol{C}_0^R$ is the fourth-order tensor of nominal instantaneous moduli. Therefore, the stability functional becomes

$$\int_{k^N V}\boldsymbol{C}_0^R(\boldsymbol{x},\boldsymbol{F})[\nabla\dot{\boldsymbol{w}}(\boldsymbol{x})]\cdot\nabla\dot{\boldsymbol{w}}(\boldsymbol{x})dV. \tag{22}$$

It turns out that a deformed state of the microstructure characterized by the fluctuation field $\boldsymbol{w}(\boldsymbol{x})$ induced by the macroscopic load $\overline{\boldsymbol{F}}$, is stable if the minimum eigenvalue of the stability functional is positive when the minimum is taken over all admissible incremental fluctuations periodic on the $k^N V$ ensemble of unit cells:

$$\Lambda(\overline{\boldsymbol{F}}) = \inf_{k\in\mathbb{N}}\left\{\min_{\dot{\boldsymbol{w}}\in H^{1,p}(k^N V_\#)}\left\{\frac{\int_{k^N V}\boldsymbol{C}_0^R(\boldsymbol{x},\overline{\boldsymbol{F}}+\nabla\boldsymbol{w}_{\overline{\boldsymbol{F}}})[\nabla\dot{\boldsymbol{w}}]\cdot\nabla\dot{\boldsymbol{w}}dV}{\int_{k^N V}\nabla\dot{\boldsymbol{w}}\cdot\nabla\dot{\boldsymbol{w}}dV}\right\}\right\} > 0. \tag{23}$$

Rigid translations, formally possible if the positive definiteness of Eq. (20) is considered as stability condition but not of interest as eigenmodes, are excluded by using condition (23). The assumed major symmetry of the microscopic moduli tensor ensures that all eigenvalues and corresponding eigenmodes of the quadratic functional are real.

The Euler–Lagrange equations and surface conditions corresponding to the above eigenvalue problem are:

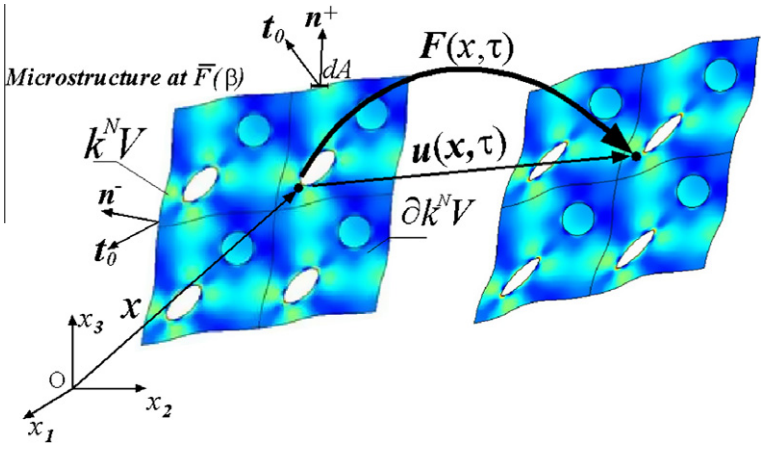

Fig. 3. Incremental deformations of the periodic microstructure described by $\boldsymbol{u}(\boldsymbol{x},\tau)$.

$$\begin{cases} div\left\{\boldsymbol{C}_0^R(\boldsymbol{x},\overline{\boldsymbol{F}}+\nabla\boldsymbol{w}_{\overline{\boldsymbol{F}}})[\nabla\dot{\boldsymbol{w}}]-\Lambda(\overline{\boldsymbol{F}})\nabla\dot{\boldsymbol{w}}\right\}=\boldsymbol{0} \text{ in } k^N V \\ \left(\left\{\boldsymbol{C}_0^R(\boldsymbol{x},\overline{\boldsymbol{F}}+\nabla\boldsymbol{w}_{\overline{\boldsymbol{F}}})[\nabla\dot{\boldsymbol{w}}]-\Lambda(\overline{\boldsymbol{F}})\nabla\dot{\boldsymbol{w}}\right\}\boldsymbol{n}\right)^+ \\ =-\left(\left\{\boldsymbol{C}_0^R(\boldsymbol{x},\overline{\boldsymbol{F}}+\nabla\boldsymbol{w}_{\overline{\boldsymbol{F}}})[\nabla\dot{\boldsymbol{w}}]-\Lambda(\overline{\boldsymbol{F}})\nabla\dot{\boldsymbol{w}}\right\}\boldsymbol{n}\right)^- \text{ on } \partial k^N V \\ \left\{\boldsymbol{C}_0^R(\boldsymbol{x},\overline{\boldsymbol{F}}+\nabla\boldsymbol{w}_{\overline{\boldsymbol{F}}})[\nabla\dot{\boldsymbol{w}}]-\Lambda(\overline{\boldsymbol{F}})\nabla\dot{\boldsymbol{w}}\right\}\boldsymbol{n}=\boldsymbol{0} \text{ on } \partial H \end{cases} \tag{24}$$

where $\boldsymbol{n}$ is the outward normal to the boundary of the unit cell assembly in the current configuration $k^N V$. The second and third equations in (24) represent the antiperiodicity condition and the free surface conditions on the hole boundary for the equivalent traction $\left\{\boldsymbol{C}_0^R(\boldsymbol{x},\overline{\boldsymbol{F}}+\nabla\boldsymbol{w}_{\overline{\boldsymbol{F}}})[\nabla\dot{\boldsymbol{w}}]-\Lambda(\overline{\boldsymbol{F}})\nabla\dot{\boldsymbol{w}}\right\}\boldsymbol{n}$, respectively.

The stability condition (23) can be also formulated with reference to the initial configuration $k^N V_{(i)}$ as:

$$\Lambda(\overline{\boldsymbol{F}})=\inf_{k\in\mathbb{N}}\left\{\min_{\dot{\boldsymbol{w}}\in H^{1,p}(k^N V_{(i)}\#)}\left\{\frac{\int_{k^N V_{(i)}}\boldsymbol{C}^R(\boldsymbol{x},\overline{\boldsymbol{F}}+\nabla\boldsymbol{w}_{\overline{\boldsymbol{F}}})[\nabla_{(i)}\dot{\boldsymbol{w}}(\boldsymbol{X})]\cdot\nabla_{(i)}\dot{\boldsymbol{w}}(\boldsymbol{X})dV_{(i)}}{\int_{k^N V_{(i)}}\nabla_{(i)}\dot{\boldsymbol{w}}(\boldsymbol{X})\cdot\nabla_{(i)}\dot{\boldsymbol{w}}(\boldsymbol{X})dV_{(i)}}\right\}\right\} >0, \tag{25}$$

where $\nabla_{(i)}\dot{\boldsymbol{w}}(\boldsymbol{X})=\partial\dot{\boldsymbol{w}}(\boldsymbol{X})/\partial\boldsymbol{X}$. This alternative formulation is useful in view of a numerical solution procedure based on a full Lagrangian approach. As a matter of fact, the stability functional equation (22) can be written in the following equivalent form with reference to the initial configuration:

$$\int_{k^N V_{(i)}}\boldsymbol{C}^R(\boldsymbol{X},\boldsymbol{F})[\nabla_{(i)}\dot{\boldsymbol{w}}(\boldsymbol{X})]\cdot\nabla_{(i)}\dot{\boldsymbol{w}}(\boldsymbol{X})dV_{(i)},$$

due to the relations between the instantaneous and fixed-reference moduli and between the deformation gradient rate and velocity gradient rate:

$$C^R_{0\,ijkl}=\frac{1}{\det\boldsymbol{F}}F_{jm}F_{ln}C^R_{imkn},\quad \dot{\boldsymbol{F}}=\boldsymbol{L}\boldsymbol{F}. \tag{26}$$

A typical situation occurring along a deformation path $\overline{\boldsymbol{F}}(\beta)$, with $\beta\geqslant 0$ and $\beta=0$ for $\overline{\boldsymbol{F}}=\boldsymbol{I}$, starting where the stability functional is positive definite, i.e. $\Lambda(\overline{\boldsymbol{F}}(0))>0$, is that Λ decreases and at some load level β_c (termed microscopic critical load parameter) the stability functional becomes positive semi-definite. At this load necessarily, the initially unique and stable principal solution ceases to be unique since an eigenmode (incremental periodic solution to the homogeneous problem) exists and the loss of microscopic structural stability occurs:

$$\Lambda(\beta_c)=0,\quad \Lambda(\beta)>0 \text{ for } 0\leqslant\beta<\beta_c.$$

As a consequence, the primary instability is detected when the minimum eigenvalue first vanishes. The microscopic stability region $\beta|\Lambda(\overline{\boldsymbol{F}}(\beta))>0$, inside which the fundamental periodic solution, for which all cells deform identically, is unique, establishes also the region where the one-cell standard homogenized energy is the correct one, namely $\Lambda(\overline{\boldsymbol{F}}(\beta))>0$ implies $\overline{W}(\overline{\boldsymbol{F}})=\overline{W}^1(\overline{\boldsymbol{F}})$.

2.4. Classical macroscopic stability analysis

A microscopic stability analysis along a macroscopic loading path $\overline{\boldsymbol{F}}(\beta)$, leading to determine the microscopic stability region, requires a notable computational effort, since it involves computations over a infinite domain. Therefore, it should be preferable to develop the stability analysis of the heterogeneous solid in terms of its macroscopic properties, determined by means of calculations performed on a unit cell, namely to carry out a macroscopic stability analysis which only requires the much simpler computation of the one-cell homogenized moduli through Eq. (12).

In view of its connection with the stability problem, a basic macroscopic measure of the stability of the periodic solid at the load parameter β can defined as the strong ellipticity condition of the homogenized moduli tensor:

$$\overline{\Lambda}(\overline{\boldsymbol{F}}(\boldsymbol{\beta}))=\min_{\|\bar{\boldsymbol{m}}\|=\|\bar{\boldsymbol{n}}\|=1}\left\{\overline{\boldsymbol{C}}_0^R(\overline{\boldsymbol{X}},\overline{\boldsymbol{F}})(\bar{\boldsymbol{m}}\otimes\bar{\boldsymbol{n}})\cdot\bar{\boldsymbol{m}}\otimes\bar{\boldsymbol{n}}\right\}>0 \tag{27}$$

in which the minimum is taken over all unit vectors $\bar{\boldsymbol{m}}$ and $\bar{\boldsymbol{n}}$.

In fact, the strong ellipticity of the homogenized solid moduli or, equivalently, the strict local rank-one convexity of the homogenized strain energy function ensures stability under Dirichlet boundary conditions when the macroscopic incremental moduli tensor is spatially constant, whereas the violation of its non-strict variant (non-negativeness of $\overline{\boldsymbol{\Lambda}}$ also called the Legendre–Hadamard condition) ensures instability under any boundary conditions.

It is worth noting that the extension of condition (27) to arbitrary rank tensors corresponds to the positive definiteness of the homogenized nominal moduli tensor:

$$\overline{\Lambda}^{(R)}(\overline{\boldsymbol{F}}(\boldsymbol{\beta}))=\min_{\|\bar{\boldsymbol{L}}\|=1}\left\{\overline{\boldsymbol{C}}_0^R(\overline{\boldsymbol{F}})[\bar{\boldsymbol{L}}]\cdot\bar{\boldsymbol{L}}\right\}>0, \tag{28}$$

which is too restrictive and physically unrealistic since it would imply uniqueness in corresponding boundary value problems for the homogenized solid, an unacceptable situation for non-linear deformations. Obviously, the condition (28) implies (27).

The macroscopic primary instability load associated to the stability condition (27) can be defined as:

$$\overline{\Lambda}(\beta_{cM})=0,\quad \overline{\Lambda}(\beta)>0 \text{ for } 0\leqslant\beta<\beta_{cM},$$

where β_{cM} is the macroscopic critical parameter and, consequently, the macroscopic stability region $\beta|\overline{\Lambda}(\beta) > 0$ can be determined. The critical load parameter $\beta_{cM}^{(R)}$ associated to (28) can be defined analogously.

The microscopic stability condition (23) implies the macroscopic stability condition (27), provided the microscopic material is strongly elliptic (Geymonat et al., 1993):

$$\min_{\|\boldsymbol{m}\|=\|\boldsymbol{n}\|=1}\left\{\boldsymbol{C}_0^R(\boldsymbol{X},\boldsymbol{F})(\boldsymbol{m}\otimes\boldsymbol{n})\cdot\boldsymbol{m}\otimes\boldsymbol{n}\right\}>0 \;\; \forall \boldsymbol{X}\in V_{(i)} \Rightarrow \Lambda(\overline{\boldsymbol{F}}(\boldsymbol{\beta}))\leqslant\overline{\Lambda}(\overline{\boldsymbol{F}}(\boldsymbol{\beta}))\Big).$$

In addition, Geymonat et al., 1993 have shown that the primary microscopic instability along a monotonic macroscopic loading process can be detected as a loss of macroscopic stability (27) provided that the wavelength of the first instability is much larger than the unit cell size (global instability mode). On the contrary, when the primary microscopic instability encountered in the loading process has a wavelength comparable to the unit cell size (local instability), the macroscopic stability condition (27) still holds and the one-cell homogenized moduli remains strongly elliptic:

$$\Lambda(\overline{\boldsymbol{F}}(\beta_c))=0\Rightarrow\begin{cases}\textit{local}\text{ instability }\overline{\Lambda}(\overline{\boldsymbol{F}}(\beta_c))>0\\ \textit{global}\text{ instability }\overline{\Lambda}(\overline{\boldsymbol{F}}(\beta_c))=0\end{cases}.$$

2.5. Macroscopic constitutive stability measures

The previous section shows that the macroscopic stability condition based on the strong ellipticity of the homogenized moduli tensor, is able to exactly predict the onset of microscopic instability of the periodic principal solution along a monotonic loading process, when the microscopic instability mode is global in nature. On the other hand, an unconservative estimation of the primary microscopic instability load is obtained in the more general case when the instability mode is of local kind, since the homogenized moduli tensor remains strongly elliptic at the onset of the primary microscopic instability.

To this aim, novel macroscopic stability measures are here introduced as an alternative approach to investigate the microscopic stability problem in terms of the homogenized properties of the periodic heterogeneous solid. Their ability to obtain conservative prediction of the primary instability load of the microstructure will be investigated in the sequel of the paper.

The incremental material response at a point $\boldsymbol{x}$ of the microstructure, Eq. (21), can be alternatively formulated by using the concept of the work conjugate stress–strain measure pairs $(\boldsymbol{T}_f,\boldsymbol{S}(\boldsymbol{U}))$ based on strain measures coaxial with $\boldsymbol{U}$, the right stretch tensor associated to $\boldsymbol{F}$, and having principal values $f(\lambda_i)$, with f a monotonic increasing function of the principal values λ_i of $\boldsymbol{U}$ such that $f(1)=0$ and $df/d\lambda_i(1)=1$ (Hill, 1968). This leads to:

$$\dot{\boldsymbol{T}}_{f(0)}=\boldsymbol{C}_0^f(\boldsymbol{X},\boldsymbol{F})[\boldsymbol{D}], \tag{29}$$

where $\dot{\boldsymbol{T}}_{f(0)}$ and $\boldsymbol{D}$ are the stress rate and the strain rate, respectively, taken with the reference configuration coinciding with the current one, corresponding to the work conjugate stress–strain measure pair $(\boldsymbol{T}_f,\boldsymbol{S}(\boldsymbol{U}))$ and is the associated fourth-order tensor of instantaneous moduli, which generally depends on the current deformation state in V. The rate of strain $\boldsymbol{D}$ equals the symmetric part of the velocity gradient $\boldsymbol{L}=\partial\boldsymbol{v}/\partial\boldsymbol{x}$ also called the Eulerian strain rate.

By using the following expression involving the rate of the first Piola–Kirchhoff stress tensor $\boldsymbol{T}_R$ to $\dot{\boldsymbol{T}}_{f(0)}$ (Ogden, 1984), evaluated when the reference configuration coincides with the current one:

$$\dot{\boldsymbol{T}}_{R(0)}=\dot{\boldsymbol{T}}_{f(0)}+\frac{1}{2}[f''(1)-1](\boldsymbol{T}_0\boldsymbol{D}+\boldsymbol{D}\boldsymbol{T}_0)+\boldsymbol{L}\boldsymbol{T}_0, \tag{30}$$

the fourth-order tensor of instantaneous moduli $\boldsymbol{C}_0^f$ can be easily related to the fourth-order tensor of nominal instantaneous moduli $\boldsymbol{C}_0^R$. The prime over $f(\lambda)$ denotes differentiation with respect to λ.

A well-known sub-class $(\boldsymbol{T}^{(\mathrm{m})},\boldsymbol{E}^{(\mathrm{m})})$ of stress–strain measure pairs can be obtained by choosing $f(\lambda_i)=(\lambda_i^m-1)/m$, where m is an integer (Ogden, 1984). The stress–strain pairs associated to the logarithmic $(\boldsymbol{E}^{(0)}=\ln\boldsymbol{U})$, the Green–Lagrange $(\boldsymbol{E}^{(2)}=\boldsymbol{U}^2-1)$ and the Biot strain $(\boldsymbol{E}^{(1)}=\boldsymbol{U}-1)$ measures, can be determined by taking $m\to 0$, $m=2$ and $m=1$, respectively. The corresponding moduli tensor are denoted as $\boldsymbol{C}_0^{(0)}$, $\boldsymbol{C}_0^{(2)}$ and $\boldsymbol{C}_0^{(1)}$, respectively. In addition the strain measure $\boldsymbol{E}^{(-2)}$ is usually attributed to Almansi and the corresponding moduli tensor is denoted by $\boldsymbol{C}_0^{(-2)}$.

According to the above representation of the microscopic constitutive response, the following family of macroscopic constitutive inequalities is introduced:

$$\overline{\Lambda}^f(\overline{\boldsymbol{F}}(\beta))=\min_{\|\overline{\boldsymbol{D}}\|=1}\left\{\overline{\boldsymbol{C}}_0^f(\overline{\boldsymbol{F}})[\overline{\boldsymbol{D}}]\cdot\overline{\boldsymbol{D}}\right\}>0, \tag{31}$$

where $\overline{\boldsymbol{D}}$ is a symmetric tensor and $\overline{\boldsymbol{C}}_0^f$ is the macroscopic tensor of instantaneous homogenized moduli which relates the macrostrain rate to the rate of the macrostress tensor $\dot{\overline{\boldsymbol{T}}}_{f(0)}$. The macroscopic tensor of instantaneous homogenized moduli $\overline{\boldsymbol{C}}_0^f$ is associated to the macroscopic strain measures $\overline{\mathrm{S}}(\overline{\boldsymbol{U}})$ defined by the classic continuum relations in terms of macroscopic quantities, where $\overline{\boldsymbol{U}}$ is the macroscopic right stretch tensor in the polar decomposition of the macroscopic deformation gradient $\overline{\boldsymbol{F}}=\overline{\boldsymbol{R}}\overline{\boldsymbol{U}}$, $\overline{\boldsymbol{R}}$ denoting the macroscopic rotation tensor.

The family of positive definiteness conditions (31) for the incremental macroscopic response, can be obtained by examining the stability condition of an equilibrium configuration for a macroscopic homogenized material element, homogeneously deformed and subjected to special macroscopic boundary conditions of traction. This condition arises in the problem of the so-called "material" or "constitutive" stability (Greco and Luciano, 2005, where the material stability condition is formulated for a material element of a homogeneous body). As a consequence, the inequalities (31) are referred to as "macroscopic constitutive stability measures".

In order to derive explicitly conditions (31), the infinitesimal stability condition of a homogeneously deformed and uniformly stressed material element, extracted from the homogenized macrocontinuum in the neighborhood of a generic interior body point $\bar{\boldsymbol{x}}(\overline{\boldsymbol{X}})$, is examined, according to arguments similar to those adopted in Greco and Luciano, 2005. The homogenized stress and strain states are assumed uniform (within the scale of variation of l_{macro}) and equal to those acting at the examined point of the macrocontinuum, under the assumption of a sufficiently small volume of the material element. The homogenized material element in the current configuration $\overline{M}$ is loaded by the traction $\overline{\boldsymbol{T}}_0\bar{\boldsymbol{n}}$ on the boundary $\partial\overline{M}$ and the uniform macroscopic stress state is specified in terms of the Cauchy stress tensor $\overline{\boldsymbol{T}}_0$.

The stability condition requires the superimposition of an incremental macroscopic displacement field $\bar{\boldsymbol{u}}(\bar{\boldsymbol{x}},\tau)=\bar{\boldsymbol{v}}(\bar{\boldsymbol{x}})\tau+\boldsymbol{o}(\tau)$ to the current configuration of the homogenized material element. Its gradient $\overline{\boldsymbol{L}}=\partial\bar{\boldsymbol{v}}/\partial\bar{\boldsymbol{x}}$ is assumed to be uniform and $\overline{M}$ is taken as the reference configuration for the subsequent deformation. The loading mechanism of the homogenized material element is represented by deformation dependent surface tractions per unit area of $\partial\overline{M}$, denoted by $\bar{\boldsymbol{t}}_R^*$, corresponding to the uniform macrostress state $\overline{\boldsymbol{T}}_0$ in the equilibrium configuration $\overline{M}$. To obtain a constitutive stability condition, these surface tractions must be defined in such a way to do not work on material rotations during additional deformation $\bar{\boldsymbol{u}}(\bar{\boldsymbol{x}},\tau)$.

The analytical expression for the surface macrotractions $\bar{\boldsymbol{t}}_R^*$, can be obtained introducing the uniform stress tensor $\overline{\boldsymbol{T}}_R^*$, representing a fictitious first Piola–Kirchhoff macrostress tensor in static equi-

librium with $\bar{\boldsymbol{t}}_R^*$, and such that the following stress power identity is satisfied:

$$\overline{\boldsymbol{T}}_R^* \cdot \dot{\overline{\boldsymbol{F}}} = \overline{\boldsymbol{T}}_0 \cdot \dot{\overline{\mathscr{F}}}(\overline{\boldsymbol{U}}) \quad \forall \bar{\boldsymbol{u}}(\bar{\boldsymbol{x}}, \tau). \tag{32}$$

Equilibrium in $\overline{M}$ requires that $\overline{\boldsymbol{T}}_R^*$ at $\tau = 0$ is equal to $\overline{\boldsymbol{T}}_0$. Therefore $\overline{\boldsymbol{T}}_R^*$ is assumed to depend on the deformation gradient and the initial stress state $\overline{\boldsymbol{T}}_0$, namely $\overline{\boldsymbol{T}}_R^*$ corresponds to a system of follower surface tractions.

The first-order approximation of Eq. (32) gives the corresponding first-order approximation of $\overline{\boldsymbol{T}}_R^*$ at $\tau = 0$:

$$\overline{\boldsymbol{T}}_R^* = \overline{\boldsymbol{T}}_0 + \left\{\frac{1}{2}[f''(1) - 1](\overline{\boldsymbol{D}}\overline{\boldsymbol{T}}_0 + \overline{\boldsymbol{T}}_0\overline{\boldsymbol{D}}) + \overline{\boldsymbol{L}}\overline{\boldsymbol{T}}_0\right\}\tau + \boldsymbol{o}(\tau). \tag{33}$$

The positiveness conditions (31) can be obtained by the second-order expansion in τ of the difference between the internal deformation work and the work done by the surface macrotraction $\bar{\boldsymbol{t}}_R^* = \overline{\boldsymbol{T}}_R^*\bar{\boldsymbol{n}}$ (with $\overline{\boldsymbol{T}}_R^*$ given by Eq. (33)) during the superposed incremental displacement $\bar{\boldsymbol{u}}(\bar{\boldsymbol{x}}, \tau)$:

$$\begin{aligned}\overline{W} - \overline{L} &= \int_0^t \left\{\int_{\overline{M}} \overline{\boldsymbol{T}}_R(\boldsymbol{\tau}) \cdot \dot{\overline{\boldsymbol{F}}}(\tau) d\upsilon - \int_{\partial\overline{M}} \overline{\boldsymbol{T}}_R^*\bar{\boldsymbol{n}} \cdot \dot{\bar{\boldsymbol{u}}}(\bar{\boldsymbol{x}}, \boldsymbol{\tau}) ds\right\} d\tau \\ &= \int_0^t \left\{\left[\overline{\boldsymbol{T}}_R(\boldsymbol{\tau}) - \overline{\boldsymbol{T}}_R^*(\boldsymbol{\tau})\right] \cdot \dot{\overline{\boldsymbol{F}}}(\tau)\right\} Vol(\overline{M}) d\boldsymbol{\tau}.\end{aligned} \tag{34}$$

On the contrary, the macroscopic condition (28) can be obtained when dead loading $\bar{\boldsymbol{t}}_R^* = \overline{\boldsymbol{T}}_0\bar{\boldsymbol{n}}$ acts during the additional deformation. In this circumstance, geometrical effects related to material rotations arise, since dead loads can do work even in a pure rotation, and we arrive at the following condition for stability:

$$\int_{\overline{M}} \dot{\overline{\boldsymbol{T}}}_R \cdot \overline{\boldsymbol{L}} d\upsilon = \dot{\overline{\boldsymbol{T}}}_R \cdot \overline{\boldsymbol{L}} Vol(\overline{M}) > 0 \ \forall \overline{\boldsymbol{L}} \neq \boldsymbol{0}, \tag{35}$$

leading to Eq. (28). This condition does not correspond to a macroscopic stability measure of constitutive type. In fact, by using Eq. (30), it is easy to show that such condition can be violated if $\overline{\boldsymbol{L}}$ coincides with an infinitesimal rotation ($\overline{\boldsymbol{L}} = \overline{\boldsymbol{W}}$). In Eq. (35), $Vol(\overline{M})$ denotes the volume of the macroscopic material element.

It is worth noting that also the macroscopic stability condition Eq. (27) can be considered as a constitutive stability condition for a homogeneous material both in the context of wave propagation and strain localization (Greco, 2007).

A macroscopic stability analysis performed by using Eq. (31), which restricts the analysis to symmetric incremental deformation gradients, leads avoiding rigid rotations, irrelevant from the physical point of view. Consequently, the macroscopic stability conditions introduced by Eq. (31), applied to symmetric incremental deformation gradients, are well distinguished from the macroscopic condition (28) extended to arbitrary incremental deformation gradients.

A consistent macroscopic stability analysis implies the assumption of a specific macroscopic strain measure in Eq. (31). As will be shown in the sequel via numerical applications, the effectiveness of a macroscopic stability measure to predict the microscopic stability behavior of the solid, depends strictly on the adopted strain measure.

If the macroscopic Biot strain tensor is used, Eq. (31) specializes to the following positivity condition:

$$\overline{\Lambda}^{(1)}(\overline{\boldsymbol{F}}(\boldsymbol{\beta})) = \min_{\|\overline{\boldsymbol{D}}\|=1} \left\{\overline{\boldsymbol{C}}_0^{(1)}(\overline{\boldsymbol{F}})[\overline{\boldsymbol{D}}] \cdot \overline{\boldsymbol{D}}\right\} > 0. \tag{36}$$

On the other hand, the use of the macroscopic logarithmic strain measure leads to:

$$\overline{\Lambda}^{(0)}(\overline{\boldsymbol{F}}(\boldsymbol{\beta})) = \min_{\|\overline{\boldsymbol{D}}\|=1} \left\{\overline{\boldsymbol{C}}_0^{(0)}(\overline{\boldsymbol{F}})[\overline{\boldsymbol{D}}] \cdot \overline{\boldsymbol{D}}\right\} > 0. \tag{37}$$

Moreover, the choice of the macroscopic Green–Lagrange strain measure leads to:

$$\overline{\Lambda}^{(2)}(\overline{\boldsymbol{F}}(\boldsymbol{\beta})) = \min_{\|\overline{\boldsymbol{D}}\|=1} \left\{\overline{\boldsymbol{C}}_0^{(2)}(\overline{\boldsymbol{F}})[\overline{\boldsymbol{D}}] \cdot \overline{\boldsymbol{D}}\right\} > 0. \tag{38}$$

Finally, when the Almansi–Hamel strain measure is adopted, we obtain:

$$\overline{\Lambda}^{(-2)}(\overline{\boldsymbol{F}}(\boldsymbol{\beta})) = \min_{\|\overline{\boldsymbol{D}}\|=1} \left\{\overline{\boldsymbol{C}}_0^{(-2)}(\overline{\boldsymbol{F}})[\overline{\boldsymbol{D}}] \cdot \overline{\boldsymbol{D}}\right\} > 0.$$

According to its microscopic counterpart, the macroscopic primary instability load associated to the conjugated stability measures can be defined as:

$$\overline{\Lambda}^f(\beta^f_{cM}) = 0, \quad \overline{\Lambda}(\beta) > 0 \text{ for } 0 \leqslant \beta < \beta^f_{cM},$$

where β^f_{cM} is the macroscopic critical parameter and, consequently, the macroscopic stability region $\beta|\overline{\Lambda}^f(\beta) > 0$ can be determined.

In order to take advantage in numerical computations, which, being carried out by using a total Lagrangian formulation, provide directly the nominal macroscopic constitutive tensor $\overline{\boldsymbol{C}}^R$, it is useful to recall the equations necessary to compute the macroscopic constitutive tensor $\overline{\boldsymbol{C}}^f_0$. Since the overall stress and strain measures are based on the nominal stress tensor and deformation gradient (Nemat-Nasser, 1999), the components of the macroscopic constitutive tensor $\overline{\boldsymbol{C}}^f_0$ can be obtained in terms of the components of the nominal macroscopic moduli tensor by using Eq. (21) and the following usual continuum relations:

$$\begin{aligned}&\dot{\overline{\boldsymbol{T}}}_{f(0)} = \dot{\overline{\boldsymbol{T}}}_{R(0)} - \frac{1}{2}[f''(1) - 1](\overline{\boldsymbol{T}}_0\overline{\boldsymbol{D}} + \overline{\boldsymbol{D}}\overline{\boldsymbol{T}}_0) - \overline{\boldsymbol{L}}\overline{\boldsymbol{T}}_0, \\ &\overline{C}^R_{0\,ijkl} = \frac{1}{\det\overline{\boldsymbol{F}}}\overline{F}_{jm}\overline{F}_{ln}\overline{C}^R_{imkn}.\end{aligned} \tag{39}$$

This leads to:

$$\overline{C}^f_{0ijkl} = \overline{C}^R_{0ijkl} - \frac{f''(1) - 1}{4}\left(\overline{T}_{ik}\delta_{jl} + \overline{T}_{il}\delta_{kj} + \overline{T}_{lj}\delta_{ki} + \overline{T}_{kj}\delta_{li}\right) - \overline{T}_{ij}\delta_{ik},$$

where $\overline{\boldsymbol{L}}$ is the macrodeformation velocity gradient $\overline{\boldsymbol{L}} = \dot{\overline{\boldsymbol{F}}}\overline{\boldsymbol{F}}^{-1}$, $\overline{\boldsymbol{D}}$ its symmetric part and $\overline{\boldsymbol{T}}_{(0)} = \overline{J}^{-1}\overline{\boldsymbol{T}}_R\overline{\boldsymbol{F}}^T$ is the macroscopic Cauchy stress tensor. It turns out that the macroscopic constitutive stability measure (31) are expressed in terms of macroscopic properties determined by means of calculations performed on a unit cell, in line with Eq. (27).

3. Numerical procedure

The theoretical formulation given in Section 2, is now used to develop some representative numerical applications. At first the computational implementation of the stability analysis is discussed. Secondly, with reference to a specific hyperelastic constitutive law, critical load parameters associated to the microscopic and the macroscopic onset of instability are presented for different loading paths and microgeometries.

3.1. FE model

A displacement-type finite element (FE) approximation, adopting plane strain Lagrange quadratic elements, is used to discretize the stability problem of a periodic microstructure. The FE model is developed by using the commercial software COMSOL MULTIPHYSICS™.

A one-way coupled FE model is employed to compute sequentially the principal solution path for the unit cell, the incremental solutions needed to determine the homogenized tangent moduli and the minimum eigenvalue of the microscopic structural stability functional. The minimum eigenvalues of the macroscopic stability measures are then determined by postprocessing the results obtained by the first and second problems.

Assuming that the loading process produces a unique response, the variational problem (7) is discretized in order to obtain the deformed configuration of a unit cell along the principal equilibrium path for a given macroscopic loading process $\overline{\boldsymbol{F}}(\beta)$. This implies that a sequence of non-linear PDE problems arising from a discrete variation of the load parameter, is solved to compute the fluctuation field solution corresponding to each macroscopic deformation along the loading path:

$$0 \leqslant \beta \leqslant \beta_{\max}, \quad \overline{\boldsymbol{F}}(\beta) \Rightarrow \boldsymbol{w}_{\overline{\boldsymbol{F}}(\beta)}(\boldsymbol{X}) \quad \Big| \int_{V_{(i)}} \boldsymbol{T}_R(\overline{\boldsymbol{F}} + \nabla \boldsymbol{w}_{\overline{\boldsymbol{F}}}, \boldsymbol{X}) \cdot \nabla \delta \boldsymbol{w} dV_{(i)} = 0 \ \forall \delta \boldsymbol{w} \in H^{1,p}(V_{(i)\#}). \tag{40}$$

A parametric solver is adopted to find the solution to the sequence of non-linear stationary PDE problems (40) that arise when the load parameter β varies. A step size equal to $\Delta\beta = 10^{-3}$ is used to discretize the loading path.

Once the evolution of the deformed configuration is known, the distribution of tangent moduli can be determined at each point of the unit cell. Therefore incremental equilibrium (linearized) problems for the unit cell and for each unit incremental macroscopic deformation mode, $\dot{\overline{\boldsymbol{F}}} = I^{hk}, \ h,k = 1,2,3$, superimposed on the given finite deformation, are solved along the loading path by the discretization of the following variational equation:

$$\int_{V_{(i)}} \boldsymbol{C}^R(\beta, \boldsymbol{X})[\boldsymbol{I}^{hk} + \nabla \dot{\boldsymbol{w}}_{\boldsymbol{I}^{hk}}] \cdot \nabla \delta \dot{\boldsymbol{w}} dV = 0 \ \forall \delta \dot{\boldsymbol{w}} \in H^{1,p}(V_{(i)\#}).$$

The homogenized moduli are thus obtained by Eq. (12) or (14). Then the load parameter associated to the lowest zero eigenvalue of the microscopic structural stability functional (23) is computed over all possible ensembles of unit cells. The linearized eigenvalue problem with a varying domain of definition is solved in the following way. For a given ensemble of unit cells, the lowest value of β for which the minimum eigenvalue of the stability functional is zero (i.e. β_c) is calculated together with the associated eigenmode, by the discretization of the minimization problem (23), leading to:

$$\int_{k^N V} \left\{ \boldsymbol{C}_0^R(\beta, x)[\nabla \dot{\boldsymbol{w}}] - \Lambda(\overline{\boldsymbol{F}}(\beta)) \nabla \dot{\boldsymbol{w}} \right\} \cdot \nabla \delta \dot{\boldsymbol{w}} dV = 0 \ \forall \delta \dot{\boldsymbol{w}} \in H^{1,p}(k^N V \#).$$

The ensemble of unit cells is then enlarged by increasing the number k. The minimum value of β_c for all currently possible instability modes thus corresponds to the loss of microscopic stability and provides the optimal ensemble of unit cells.

On the other hand, the macroscopic stability analysis is performed by monitoring the lowest eigenvalue of the acoustic tensor $\overline{\boldsymbol{Q}}_{0ih}(\bar{\boldsymbol{n}}) = \overline{C}^R_{0ijhk} \bar{n}_j \bar{n}_k$, for every direction of propagation $\bar{\boldsymbol{n}}$:

$$\overline{\Lambda}(\overline{\boldsymbol{F}}(\beta)) = \min_i \left[\min_{\|\bar{\boldsymbol{n}}\|=1} \lambda_i^{\overline{Q}(\bar{n})}(\beta) \right] \text{ with } \lambda_i^{\overline{Q}(\bar{n})} | (\overline{\boldsymbol{Q}}_0(\bar{\boldsymbol{n}}) - \lambda_i^{\overline{Q}(\bar{n})} \boldsymbol{I}) \hat{\Phi}_i = 0.$$

For 2D problems, the orientation of the singular surface is uniquely determined by an angle θ via:

$$\bar{\boldsymbol{n}} = [\bar{n}_1 = \cos\theta, \bar{n}_2 = \sin\theta, 0] \quad 0 \leqslant \theta < 2\pi.$$

As a consequence the scan of the minimum eigenvalue is checked for θ between 0 and 2π. The first macroscopic instability is detected when the lowest eigenvalue becomes zero.

Accordingly, the onset of macroscopic instability according to the conjugated stability measures is determined by monitoring the lowest eigenvalue of (31):

$$\overline{\Lambda}^f(\overline{\boldsymbol{F}}(\beta)) = \min \left[\lambda_i^{\overline{C}^f_0}(\beta) \right],$$

with $\lambda_i^{\overline{C}^f_0}$ denoting the ith eigenvalue associated to the following algebraic eigenproblem:

$$\left(\overline{\boldsymbol{C}}^f_0 - \lambda_i^{\overline{C}^f_0} \boldsymbol{I} \right) \widehat{\underset{i}{\Phi}} = \boldsymbol{0}. \tag{41}$$

Eq. (41) is here given in matrix form for completeness:

$$\left(\begin{bmatrix} \overline{C}^f_{01111} & \overline{C}^f_{01122} & 2\overline{C}^f_{01112} \\ \overline{C}^f_{01122} & \overline{C}^f_{02222} & 2\overline{C}^f_{02212} \\ 2\overline{C}^f_{01112} & 2\overline{C}^f_{02212} & 2\overline{C}^f_{01212} \end{bmatrix} - \lambda_i^{\overline{C}^f_0} diag\{1,1,1\} \right) \begin{Bmatrix} \tilde{\Phi}^{(i)}_{11} \\ \tilde{\Phi}^{(i)}_{22} \\ \tilde{\Phi}^{(i)}_{12} \end{Bmatrix} = \begin{Bmatrix} 0 \\ 0 \\ 0 \end{Bmatrix}.$$

The onset of macroscopic instability is determined by searching for the lowest load parameter at which the lowest eigenvalue of (31) becomes zero.

Similarly, the eigenvalue problem representing the macroscopic condition (28) is:

$$\left(\begin{bmatrix} \overline{C}^R_{1111} & \overline{C}^R_{1122} & \overline{C}^R_{1112} & \overline{C}^R_{1121} \\ \overline{C}^R_{2211} & \overline{C}^R_{2222} & \overline{C}^R_{2212} & \overline{C}^R_{2221} \\ \overline{C}^R_{1211} & \overline{C}^R_{1222} & \overline{C}^R_{1212} & \overline{C}^R_{1221} \\ \overline{C}^R_{2111} & \overline{C}^R_{2122} & \overline{C}^R_{2112} & \overline{C}^R_{2121} \end{bmatrix} - \lambda_i^{\overline{C}^R} diag\{1,1,1,1\} \right) \begin{Bmatrix} \Phi^{(i)}_{11} \\ \Phi^{(i)}_{22} \\ \Phi^{(i)}_{12} \\ \Phi^{(i)}_{21} \end{Bmatrix} = \begin{Bmatrix} 0 \\ 0 \\ 0 \\ 0 \end{Bmatrix}.$$

In the framework of the finite and incremental homogenization procedure, periodic boundary conditions are implemented by means of the extrusion coupling variable methodology. According to this method, the displacement field or its increment is made available on the opposite boundary faces of the unit cell. Once the displacement field or its increment is extruded from the source domain (the negative unit cell faces $\partial V^-_{(i)}$) to the destination one (the positive unit cell faces $\partial V^+_{(i)}$), periodic boundary constraints are imposed as point constraints on the destination boundaries of the unit cell, by means of the following constraint equations:

$$\boldsymbol{u}(\boldsymbol{X}^+) = \boldsymbol{u}(\boldsymbol{X}^-) + (\overline{\boldsymbol{F}} - \boldsymbol{I})(\boldsymbol{X}^+ - \boldsymbol{X}^-),$$
$$\dot{\boldsymbol{u}}(\boldsymbol{X}^+) = \dot{\boldsymbol{u}}(\boldsymbol{X}^-) + \dot{\overline{\boldsymbol{F}}}(\boldsymbol{X}^+ - \boldsymbol{X}^-),$$

where $\boldsymbol{u}(\boldsymbol{X}^-)$ and $\dot{\boldsymbol{u}}(\boldsymbol{X}^-)$ are the displacement and the incremental displacement fields, respectively, extruded from $\partial V^-_{(i)}$. The fluctuation field is obtained by means of the following expression:

$$\boldsymbol{w}(\boldsymbol{X}) = \boldsymbol{u}(\boldsymbol{X}) - (\overline{\boldsymbol{F}} - \boldsymbol{I})\boldsymbol{X}.$$

Similar considerations can be done when periodic boundary conditions must be applied on the boundary of a unit cell assembly $k^N V$.

In order to exclude rigid body motions, the fluctuation field can be assumed to be zero at the corner points of the unit cell, implying that the displacement field at the corner points is driven by the macroscopic deformation gradient.

The microscopic and macroscopic stability analyses have been managed by developing a computer code written in the COMSOL-SCRIPT™ programming language, which is interfaced with COMSOL MULTIPHYSICS™.

3.2. Microstructural models

Although the theoretical formulation of this work is valid for materials characterized by an incrementally linear constitutive law, numerical examples are developed by adopting the experimentally based compressible Gent, 1996 constitutive law for each microconstituents. This implies that each microscopic components obeys the following strain energy density:

$$W = -\frac{\mu}{2}\left[J_m \ln\left(1 - \frac{\|\boldsymbol{F}\|^2 - 3}{J_m} \right) + 2\ln J \right] + \left(\frac{k-\mu}{2} - \frac{\mu}{J_m} \right)(J-1)^2$$

where μ and κ are the shear and bulk moduli of the solid at zero strain, respectively, J denotes $\mathrm{Det}(\boldsymbol{F})$ and J_m is a constant which calibrates the solid's strain saturation ($\boldsymbol{T}_R \to \infty$) occurring when

$\|\boldsymbol{F}\|^2 \to J_m + 3$. By assuming $\mu > 0$, $\kappa > [(J_m + 2)/J_m]\mu$, $J_m > 0$ the Gent solid becomes polyconvex and hence rank-one convex (Ball, 1977). This property excludes the onset of strain discontinuities within each phase of the deformed microstructure and ensures that the strong ellipticity condition is satisfied for the microscopic material. For the numerical calculations the values of $J_m = 50$ and $\kappa/\mu = 10$ are adopted.

In addition the neo-Hookean constitutive model is also adopted, which can be extracted by the Gent constitutive model in the limit as $J_m \to \infty$:

$$W = \frac{\mu}{2}\left[(\|\boldsymbol{F}\|^2 - 3) - 2\ln J\right] + \left(\frac{k-\mu}{2}\right)(J-1)^2.$$

Numerical calculations are performed with reference to two different types of macroscopic loading paths: an equibiaxial and uniaxial loading along the reference coordinate axes, represented, respectively, by:

$$\overline{\boldsymbol{F}}(\beta) = \begin{bmatrix} 1+\beta & 0 & 0 \\ 0 & 1+\beta & 0 \\ 0 & 0 & 1 \end{bmatrix}, \quad \overline{\boldsymbol{F}}(\beta) = \begin{bmatrix} 1+\beta & 0 & 0 \\ 0 & 1 & 0 \\ 0 & 0 & 1 \end{bmatrix}.$$

It turns out that the load parameter β coincides with the principal value of the Biot strain tensor in the X_1 direction in the uniaxial case, and with the principal values of the Biot strain tensor in the X_1 and X_2 directions, in the equibiaxial case.

For the first application, a cellular microstructure with an initial square distribution of circular voids is adopted. In the second one a particle-reinforced composite microstructure is considered, with a square distribution of inclusions, which can be considered as representative of a cross section of a fiber-reinforced solid with cylindrical fibers aligned in the X_3 axis direction.

In both cases the unit cell dimensions are $L_1 = L_2 = L$ and the radius of the voids and the inclusions is $R = 0.25L$. Hence the initial porosity equal to the volume fraction of the inclusions is $\pi/16$. In the case of the particle-reinforced composite different ratios between the material parameters of the inclusion and the matrix are adopted, namely $\mu_f/\mu_m = 0.5$ representing a soft inclusion and $\mu_f/\mu_m = 10$, $\mu_f/\mu_m = 50$ representing stiff inclusions. In the numerical calculations the shear modulus at zero strain of the matrix material has been assumed equal to $\mu = 807$ N/mm^2.

For the cellular microgeometry the mesh adopted to discretize the unit cell problem involves 15,616 degrees of freedom and 3810 quadratic Lagrangian triangular elements. In the case of the reinforced microgeometry 31,194 degrees of freedom and 7598 quadratic Lagrangian triangular elements are adopted.

The largest assembly examined to perform the microscopic stability analysis corresponds to an array of 10×10 unit cells. This assembly is assumed to reasonably approximate the theoretically infinite domain of microscopic stability analysis and to provide values of the critical load parameter in the case of a global instability mode sufficiently close to those obtained by using the macroscopic stability measure (27). Specifically, the instability mode has been classified as global, when by considering increasing unit cell assemblies, the lowest value of the load parameter for which the minimum eigenvalue of stability functional first vanishes, approaches from above the load parameter corresponding to the macroscopic loss of ellipticity, within a relative percentage error $(\beta_{cM} - \beta_c)/\beta_{cM}$ x100 equal to 1. A typical mesh of a 10x10 assembly is shown in Fig. 4, adopting 302,852 degrees of freedom and 37,716 quadratic Lagrangian triangular elements for the reinforced microgeometry and 222,644 degrees of freedom and 26,540 quadratic Lagrangian triangular elements for the cellular one.

4. Numerical applications

Numerical stability analyses are here carried out with reference to the above described microstructural models, in order to investigate the effectiveness of the macroscopic constitutive stability measures introduced in Section 2.5.

4.1. Cellular microstructure

The stability analysis of the Gent cellular microstructure is illustrated in Figs. 5 and 6 for the equibiaxial and uniaxial cases, respectively, where the primary microscopic instability modes and the critical load parameters at the onset of microscopic instability are also shown.

These results show that in compression the onset of microscopic instability (occurring at $\beta_c^- = -0.075$ in the equibiaxial case and at $\beta_c^- = -0.144$ in the uniaxial one) always precedes the macroscopic loss of strong ellipticity (i.e. the macroscopic loss of stability according to Eq. (27)) and the local microscopic instability mode is periodic on a 2×2 cell assembly. The $+(-)$ superscript attached to the critical load parameter denotes its value in tension (compression). The corresponding instability modes involve an alternation of void ovalization (see Figs. 5a and 6a).

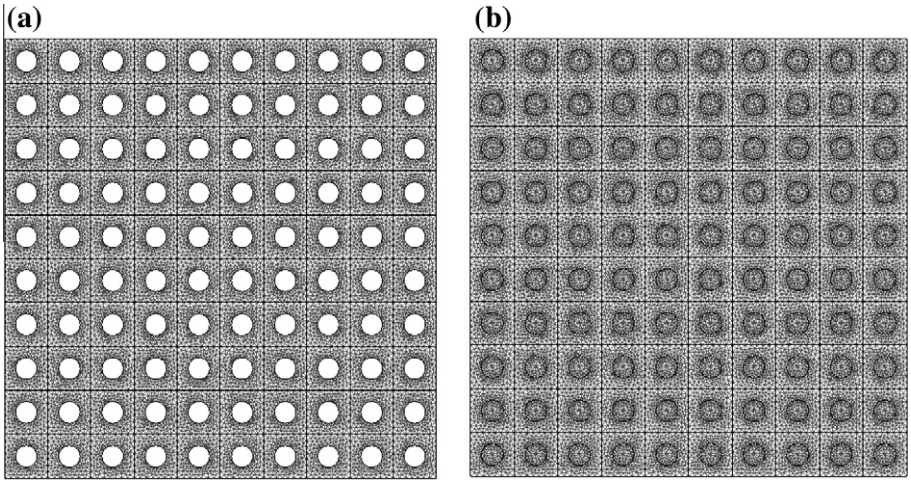

Fig. 4. Typical meshes adopted for microscopic stability analysis: (a) cellular microstructure and (b) particle-reinforced microstructure.

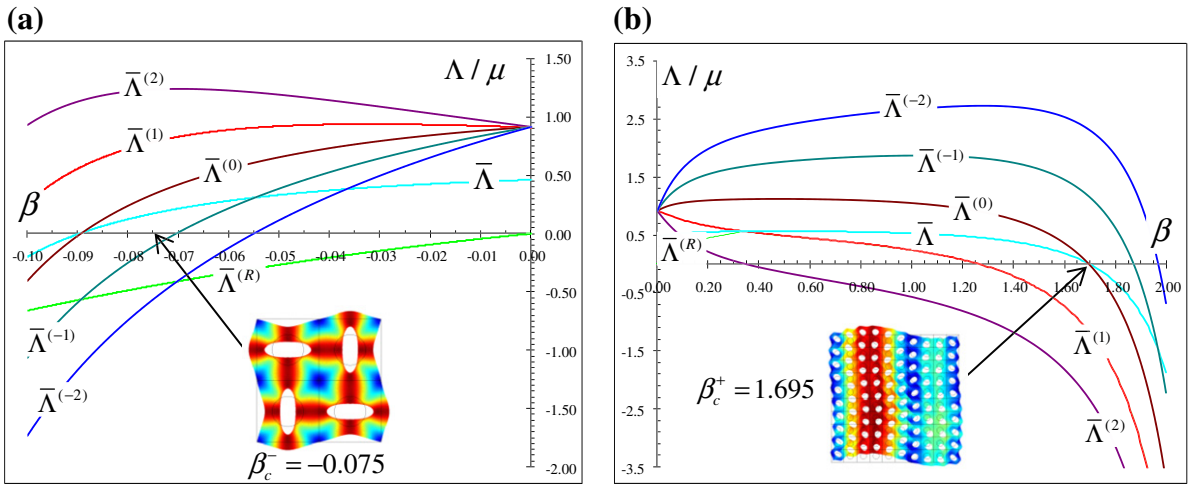

Fig. 5. Evolution of the macroscopic stability measures for a Gent cellular microstructure under equibiaxial loading with illustration of the microscopic instability loads and associated modes.

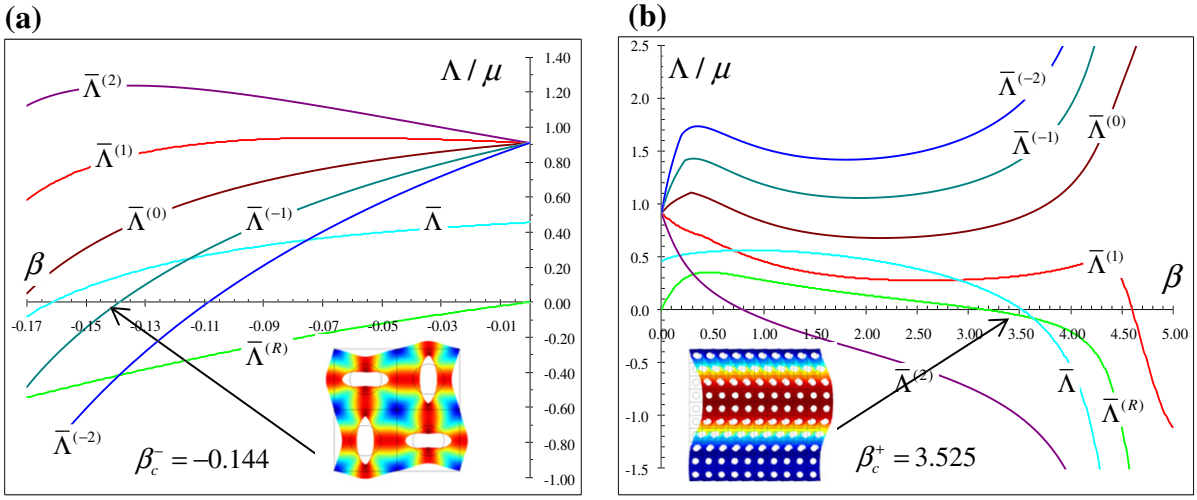

Fig. 6. Evolution of the macroscopic stability measures for a Gent cellular microstructure under uniaxial loading with illustration of the microscopic instability loads and associated modes.

In the tension case, the first instability mode is global in nature and, consequently, the macroscopic loss of stability according to Eq. (27) coincides with the microscopic one, occurring at $\beta_c^+ = 1.695$ in the equibiaxial case and at $\beta_c^+ = 3.525$ in the uniaxial case. Primary instability modes in tension, occurring with a degree of multiplicity equal to four in the equibiaxial case, are illustrated in Figs. 5b and 6b with reference to a 10×10 cell assembly.

The stability analysis carried out by using the macroscopic conjugated stability measures, shows that in tension, for the equibiaxial case, the positive definiteness conditions related to $\overline{\Lambda}^{(2)}$ and $\overline{\Lambda}^{(1)}$, are first violated before the macroscopic loss of strong ellipticity. For the uniaxial case, only the macroscopic condition $\overline{\Lambda}^{(2)}$ becomes positive-semi-definite before the macroscopic loss of strong ellipticity, whereas $\overline{\Lambda}^{(1)}$ loses its positiveness after the macroscopic loss of strong ellipticity. On the other hand, the loss of macroscopic stability according to $\overline{\Lambda}^{(-1)}$ and $\overline{\Lambda}^{(-2)}$, occur after the loss of macroscopic strong ellipticity in equibiaxial tension, while stability is always preserved in the uniaxial tension case.

In the compressive case, the situation is reversed since the loss of positive definiteness of $\overline{\Lambda}^{(-1)}$ and $\overline{\Lambda}^{(-2)}$ precedes the macroscopic loss of strong ellipticity. On the contrary, $\overline{\Lambda}^{(2)}$ and $\overline{\Lambda}^{(1)}$ remains always positive in the examined macrostrain range, although show a decreasing behavior and tend to become positive-semi-definite for larger levels of strains.

As far as the macroscopic stability measure related to $\overline{\Lambda}^{(0)}$ is concerned, in the equibiaxial case the loss of macroscopic stability coincides with the macroscopic loss of strong ellipticity, both in tension and in compression, within numerical errors related to the FE discretization. In the uniaxial case, $\overline{\Lambda}^{(0)}$ does not lose its positivity in the examined range of macrostrain, and shows an increasing behavior in tension and a decreasing one in compression.

The critical value of the load parameters for the examined stability measures are shown in Table 1.

As expected, the macroscopic stability measure (28) is violated at 0^- in compression due to rotational instabilities, and before the macroscopic condition (27) in tension.

The stability analysis for the cellular microstructure of neo-Hookean material, is illustrated in Figs. 7 and 8 for the equibiaxial and uniaxial case, respectively. Results show that the situation in compression is similar to the Gent case (the microscopic primary instability occurring at $\beta_c^- = -0.075$ in the equibiaxial case and at $\beta_c^- = -0.144$ in the uniaxial one) and the instability modes are

Table 1
Cellular microstructure of Gent material: critical load parameter values for the examined stability measures.

Tension	$\beta_{cM}^{(2)+}$	$\beta_{cM}^{(1)+}$	$\beta_{cM}^{(0)+}$	β_{c}^{+}	β_{cM}^{+}	$\beta_{cM}^{(-1)+}$	$\beta_{cM}^{(-2)+}$	$\beta_{cM}^{(R)+}$
Equibiaxial	0.345	1.255	1.695	1.695	1.695	1.875	1.965	1.255
Uniaxial	0.785	4.605	–	3.525	3.525	–	–	3.155
Compression	$\beta_{cM}^{(2)-}$	$\beta_{cM}^{(1)-}$	$\beta_{cM}^{(0)-}$	β_{c}^{-}	β_{cM}^{-}	$\beta_{cM}^{(-1)-}$	$\beta_{cM}^{(-2)-}$	$\beta_{cM}^{(R)-}$
Equibiaxial	–	–	−0.089	−0.075	−0.089	−0.070	−0.055	0
Uniaxial	–	–	–	−0.144	−0.162	−0.139	−0.109	0

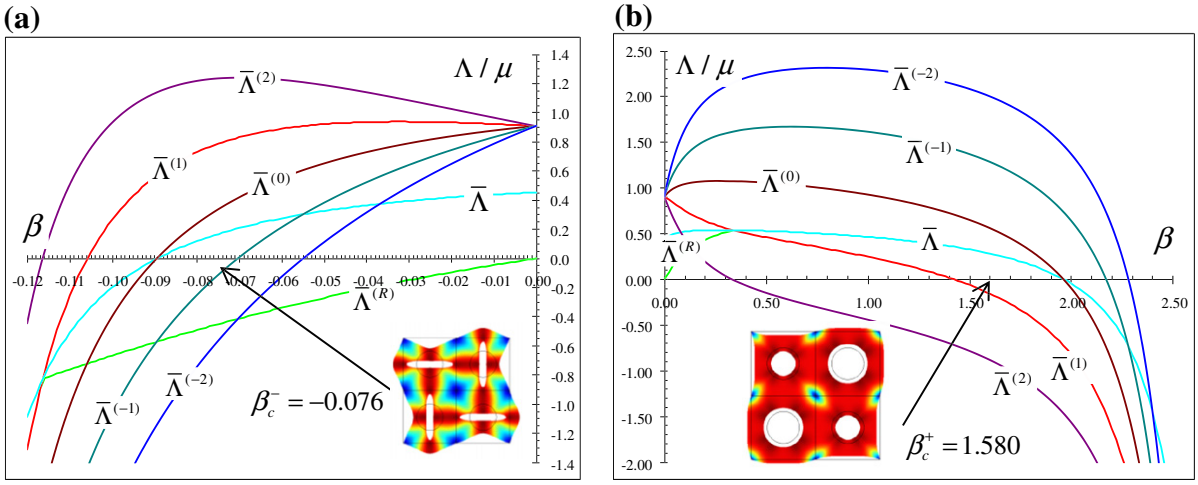

Fig. 7. Evolution of the macroscopic stability measures for a neo-Hookean cellular microstructure under equibiaxial loading with illustration of the microscopic instability loads and associated modes.

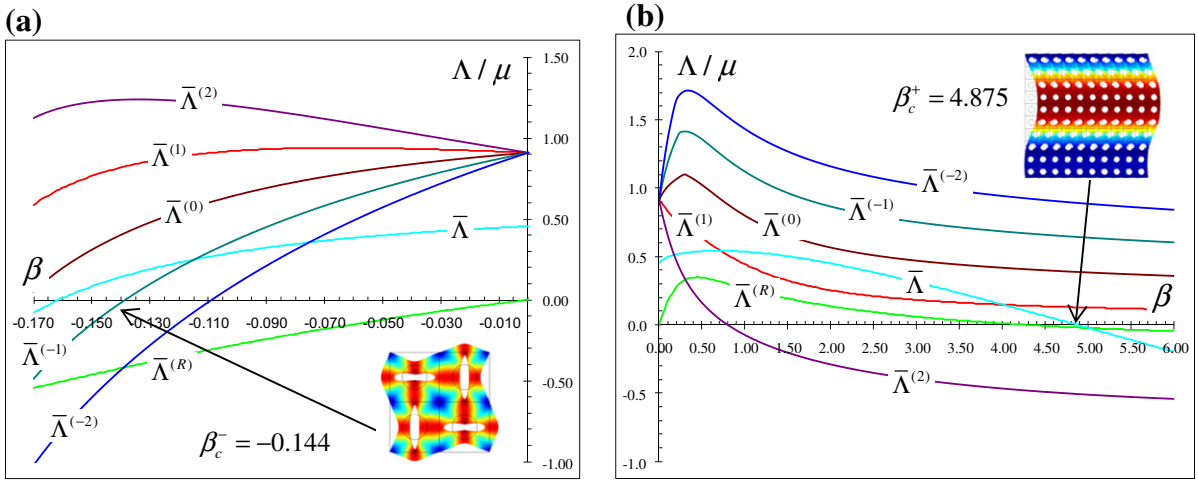

Fig. 8. Evolution of the macroscopic stability measures for a neo-Hookean cellular microstructure under uniaxial loading with illustration of the microscopic instability loads and associated modes.

of local type with periodicity on a 2×2 cell assembly (Figs. 7a and 8a).

In the tension case, the situation is somewhat different from the Gent material, since the primary instability mode is local for the equibiaxial case with a 2×2 periodicity (Fig. 7b), and global for the uniaxial one (Fig. 8b). Consequently, the macroscopic loss of stability according to Eq. (27) coincides with the microscopic one in the uniaxial case and occurs at $\beta_c^+ = 4.875$. On the contrary, in the equibiaxial case, the microscopic loss of stability, occurring at $\beta_c^+ = 1.585$, precedes the macroscopic loss of strong ellipticity.

The critical values of the load parameters for the examined stability measures are reported in Table 2. Despite the different behavior in the nature of microscopic instability modes in tension and the differences in critical load parameter values, the same considerations made in the Gent case for the macroscopic stability measures, can be applied for the neo-Hookean cellular microstructure. As a matter of fact, the sequences of critical load parameters related to the macroscopic stability measures remain practically unchanged, as can be noted by means of comparisons between Tables 1 and 2.

Table 2
Cellular microstructure of neo-Hookean material: critical load parameter values for the examined stability measures.

Tension	$\beta_{cM}^{(2)+}$	$\beta_{cM}^{(1)+}$	$\beta_{cM}^{(0)+}$	β_c^+	β_{cM}^+	$\beta_{cM}^{(-1)+}$	$\beta_{cM}^{(-2)+}$	$\beta_{cM}^{(R)+}$
Equibiaxial	0.330	1.430	1.970	1.580	1.970	2.170	2.290	1.430
Uniaxial	0.795	–	–	4.875	4.875	–	–	4.245
Compression	$\beta_{cM}^{(2)-}$	$\beta_{cM}^{(1)-}$	$\beta_{cM}^{(0)-}$	β_c^-	β_{cM}^-	$\beta_{cM}^{(-1)-}$	$\beta_{cM}^{(-2)-}$	$\beta_{cM}^{(R)-}$
Equibiaxial	−0.117	−0.106	−0.090	−0.076	−0.090	−0.071	−0.055	0
Uniaxial	–	–	–	−0.144	−0.162	−0.139	−0.109	0

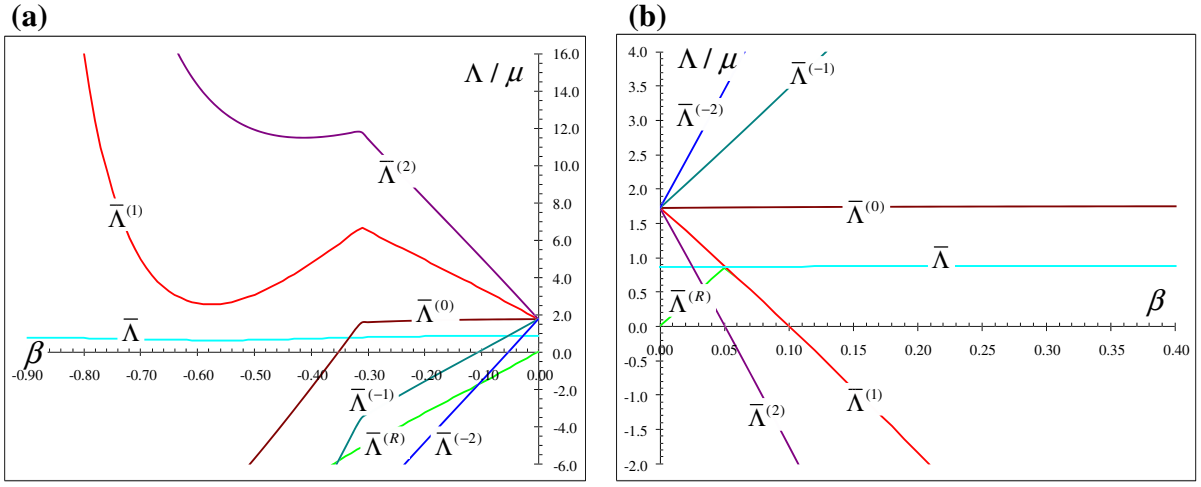

Fig. 9. Stability analysis of a particle-reinforced microstructure of Gent material under equibiaxial loading, $\mu_f/\mu_m = 0.5$.

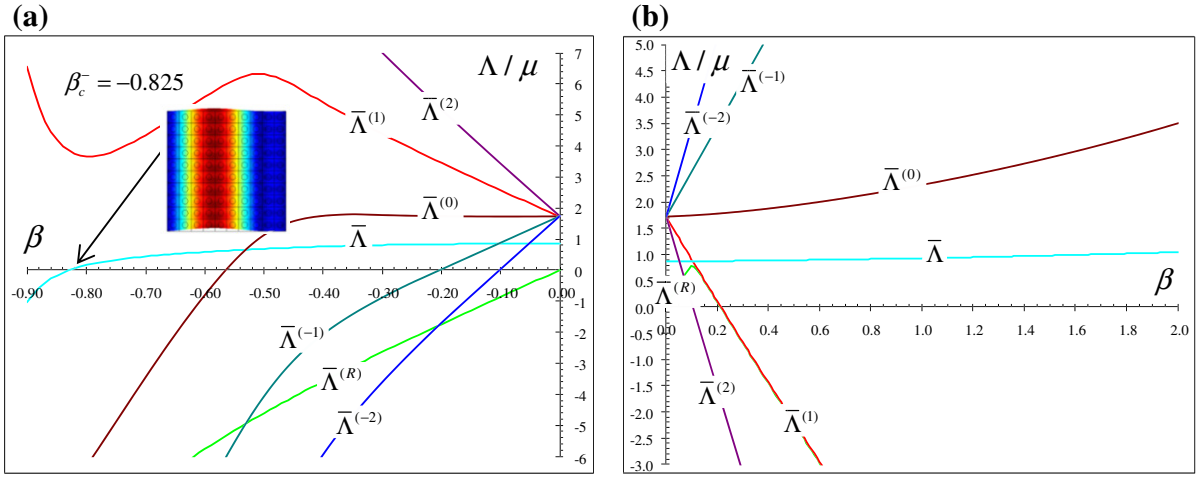

Fig. 10. Stability analysis of a particle-reinforced microstructure of Gent material under uniaxial loading, $\mu_f/\mu_m = 0.5$.

The above results show that the $\overline{\Lambda}^{(2)}$ condition provides conservative estimates of the primary microscopic instability load in tension, whereas the conditions $\overline{\Lambda}^{(-1)}$ and $\overline{\Lambda}^{(-2)}$ are able provide conservative predictions in compression, namely the following inequalities are always valid:

$$\beta_{cM}^{(2)+} < \beta_c^+$$
$$\beta_c^- < \beta_{cM}^{(-1)-} < \beta_{cM}^{(-2)-}.$$

On the other hand, the $\overline{\Lambda}^{(1)}$ condition is able to provide conservative predictions only in the equibiaxial case. It is worth noting that in the equibiaxial case the $\overline{\Lambda}^{(0)}$ condition gives an exact prediction of the microscopic instability, whereas in the uniaxial case the $\overline{\Lambda}^{(0)}$ condition gives an unconservative microscopic instability load prediction.

Among the proposed conjugated stability measures, the $\overline{\Lambda}^{(1)}$ and the $\overline{\Lambda}^{(-1)}$ conditions give the less conservative prediction of the microscopic critical load parameter in tension and compression for the equibiaxial case, respectively. On the other hand, the less conservative predictions for the uniaxial case in tension and compression are provided by $\overline{\Lambda}^{(2)}$ and $\overline{\Lambda}^{(-1)}$, respectively.

Finally, in tension the condition (28) gives conservative estimate of the microscopic critical load parameter. This situation always occurs when the instability mode is global in nature since

Table 3
Particle-reinforced microstructure of Gent material: critical load parameter values.

(a) $\mu_f/\mu_m = 0.5$ Tension	$\beta_{cM}^{(2)+}$	$\beta_{cM}^{(1)+}$	$\beta_{cM}^{(0)+}$	β_c^+	β_{cM}^+	$\beta_{cM}^{(-1)+}$	$\beta_{cM}^{(-2)+}$	$\beta_{cM}^{(R)+}$
Equibiaxial	0.055	0.105	–	–	–	–	–	0.105
Uniaxial	0.105	0.215	–	–	–	–	–	0.215
Compression	$\beta_{cM}^{(2)-}$	$\beta_{cM}^{(1)-}$	$\beta_{cM}^{(0)-}$	β_c^-	β_{cM}^-	$\beta_{cM}^{(-1)-}$	$\beta_{cM}^{(-2)-}$	$\beta_{cM}^{(R)-}$
Equibiaxial	–	–	−0.355	–	–	−0.105	−0.055	0
Uniaxial	–	–	−0.565	−0.825	−0.825	−0.205	−0.105	0
(b) $\mu_f/\mu_m = 10$ Tension	$\beta_{cM}^{(2)+}$	$\beta_{cM}^{(1)+}$	$\beta_{cM}^{(0)+}$	β_c^+	β_{cM}^+	$\beta_{cM}^{(-1)+}$	$\beta_{cM}^{(-2)+}$	$\beta_{cM}^{(R)+}$
Equibiaxial	0.055	0.105	–	–	–	–	–	0.105
Uniaxial	0.105	0.215	–	–	–	–	–	0.215
Compression	$\beta_{cM}^{(2)-}$	$\beta_{cM}^{(1)-}$	$\beta_{cM}^{(0)-}$	β_c^-	β_{cM}^-	$\beta_{cM}^{(-1)-}$	$\beta_{cM}^{(-2)-}$	$\beta_{cM}^{(R)-}$
Equibiaxial	–	–	−0.545	−0.545	−0.545	−0.105	−0.055	0
Uniaxial	–	–	–	−0.475	−0.475	−0.205	−0.105	0
(c) $\mu_f/\mu_m = 50$ Tension	$\beta_{cM}^{(2)+}$	$\beta_{cM}^{(1)+}$	$\beta_{cM}^{(0)+}$	β_c^+	β_{cM}^+	$\beta_{cM}^{(-1)+}$	$\beta_{cM}^{(-2)+}$	$\beta_{cM}^{(R)+}$
Equibiaxial	0.055	0.105	–	–	–	–	–	0.105
Uniaxial	0.105	0.225	–	–	–	–	–	0.215
Compression	$\beta_{cM}^{(2)-}$	$\beta_{cM}^{(1)-}$	$\beta_{cM}^{(0)-}$	β_c^-	β_{cM}^-	$\beta_{cM}^{(-1)-}$	$\beta_{cM}^{(-2)-}$	$\beta_{cM}^{(R)-}$
Equibiaxial	–	−0.585	−0.475	−0.475	−0.475	−0.105	−0.055	0
Uniaxial	–	–	−0.535	−0.415	−0.415	−0.205	−0.105	0

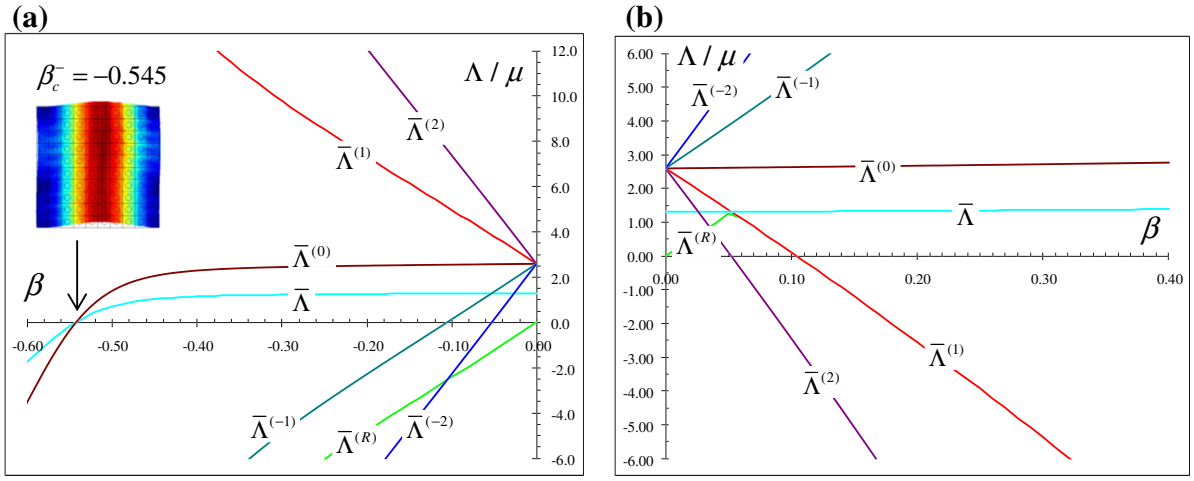

Fig. 11. Stability analysis of a particle-reinforced microstructure of Gent material under equibiaxial loading, $\mu_f/\mu_m = 10$.

condition (28) always implies (27). In addition, it can be noted that in the equibiaxial case the loss of macroscopic stability according to the condition (28) occurs with a symmetric incremental deformation gradient (***L=D***) and, consequently, it coincides with the loss of positivity of $\overline{\Lambda}^{(1)}$.

4.2. Particle-reinforced microstructure

In the case of the particle-reinforced microstructure with different stiffness contrasts between the inclusion and the matrix ($\mu_f/\mu_m = 0.5$, 10, 50), the main difference with respect to the cellular microstructure in the stability analysis, is that in the compression case the first microscopic instability mode is always of global type and coincides with the macroscopic instability related to the strong ellipticity condition. The only exception is the case $\mu_f/\mu_m = 0.5$ where microscopic stability is always preserved. On the other hand, in tension the microstructure is always stable for the examined range of deformations.

The stability analysis developed for the $\mu_f/\mu_m = 0.5$ case, is illustrated in Figs. 9 and 10 and shows that the onset of microscopic instability occurs only in compression for the uniaxial loading condition at $\beta_c^- = -0.825$ with two simultaneous modes. One of the two simultaneous microscopic instability mode, all of global type, is shown in Fig. 10a.

In compression, the loss of positivity is exhibited only by $\overline{\Lambda}^{(-2)}$, $\overline{\Lambda}^{(-1)}$ and $\overline{\Lambda}^{(0)}$, whereas in tension it occurs only for $\overline{\Lambda}^{(2)}$, $\overline{\Lambda}^{(1)}$ and $\overline{\Lambda}^{(R)}$. The critical value of the load parameters are shown in Table 3a. When microscopic instability occurs, the condition $\overline{\Lambda}^{(-2)}$, $\overline{\Lambda}^{(-1)}$ and $\overline{\Lambda}^{(0)}$ are able to provide conservative stability predictions with the less conservative one given by $\overline{\Lambda}^{(0)}$.

The stability analysis for $\mu_f/\mu_m = 10$, illustrated in Figs. 11 and 12, shows that in compression the onset of microscopic

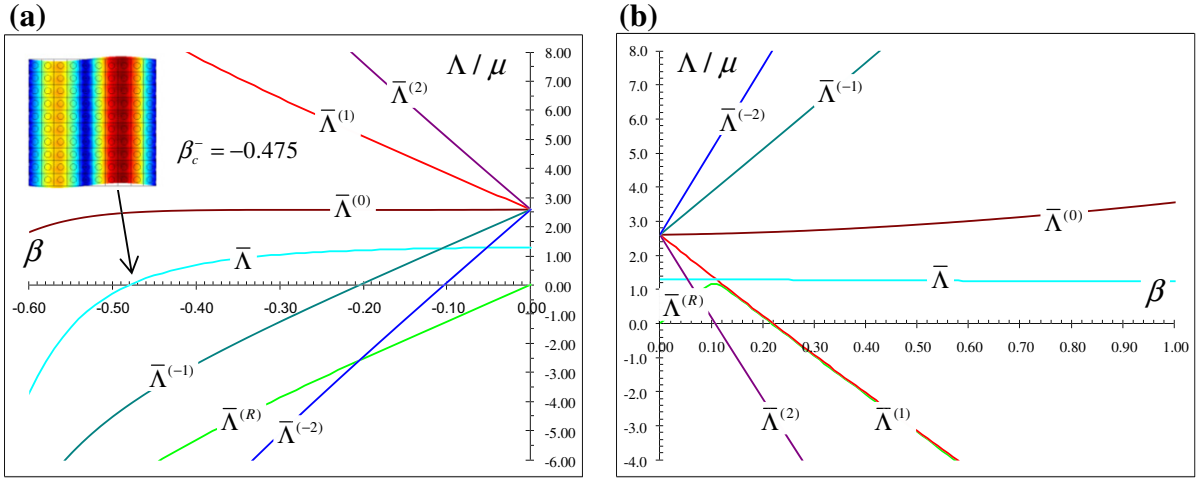

Fig. 12. Stability analysis of a particle-reinforced microstructure of Gent material under uniaxial loading, $\mu_f/\mu_m = 10$.

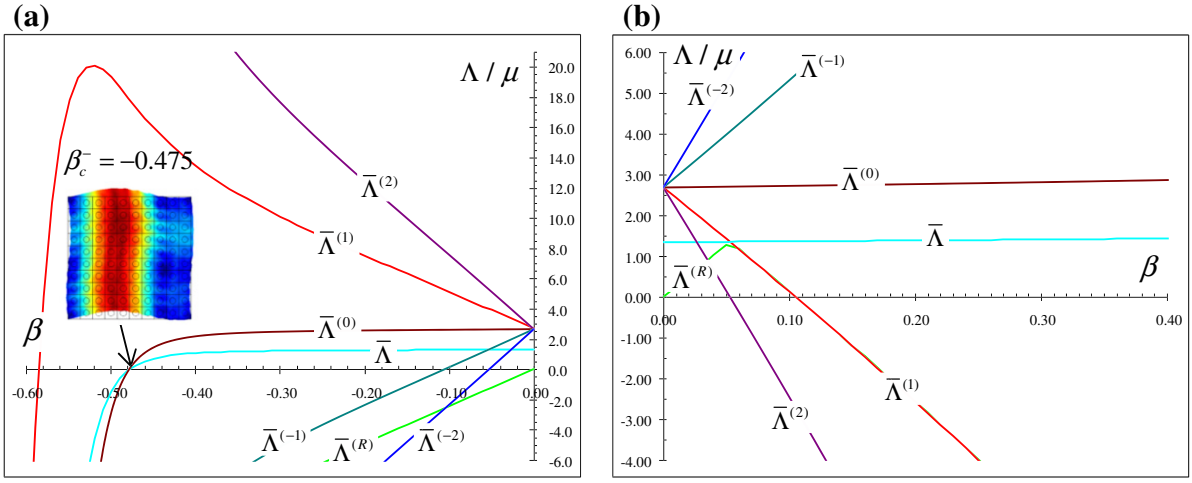

Fig. 13. Stability analysis of a particle-reinforced microstructure of Gent material under equibiaxial loading, $\mu_f/\mu_m = 50$.

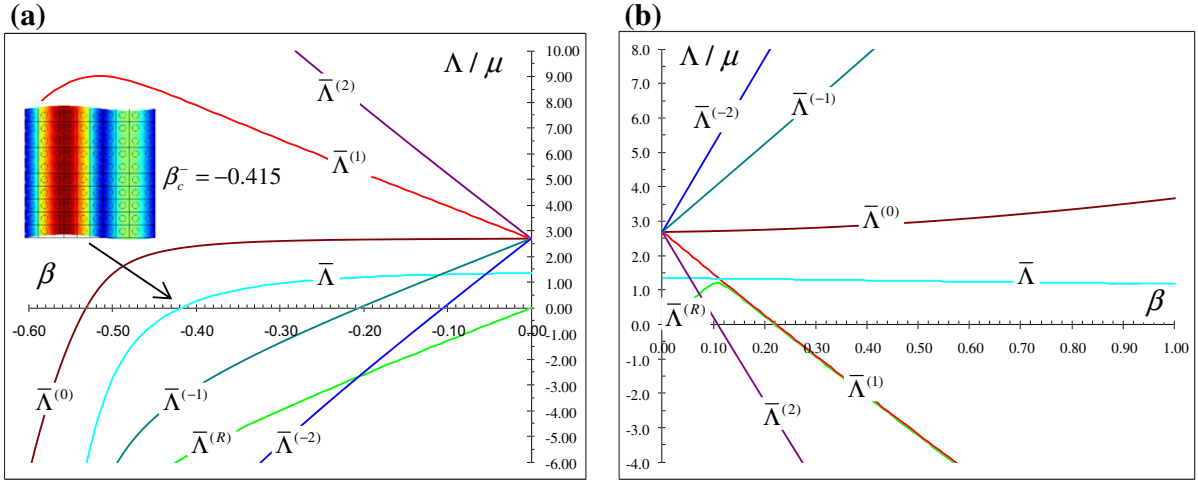

Fig. 14. Stability analysis of a particle-reinforced microstructure of Gent material under uniaxial loading, $\mu_f/\mu_m = 50$.

instability occurs at $\beta_c^- = -0.545$ in the equibiaxial case and at $\beta_c^- = -0.475$ in the uniaxial one. Figs. 11a and 12a show one of the four simultaneous modes occurring in the equibiaxial compression case and one of the two simultaneous modes occurring in the uniaxial compression case, respectively.

Table 4
Particle-reinforced microstructure of neo-Hookean material: critical load parameter values.

(a) $\mu_f/\mu_m = 0.5$ Tension	$\beta_{cM}^{(2)+}$	$\beta_{cM}^{(1)+}$	$\beta_{cM}^{(0)+}$	β_c^+	β_{cM}^+	$\beta_{cM}^{(-1)+}$	$\beta_{cM}^{(-2)+}$	$\beta_{cM}^{(R)+}$
Equibiaxial	0.055	0.105	–	–	–	–	–	0.105
Uniaxial	0.105	0.215	–	–	–	–	–	0.215
Compression	$\beta_{cM}^{(2)-}$	$\beta_{cM}^{(1)-}$	$\beta_{cM}^{(0)-}$	β_c^-	β_{cM}^-	$\beta_{cM}^{(-1)-}$	$\beta_{cM}^{(-2)-}$	$\beta_{cM}^{(R)-}$
Equibiaxial	–	–	−0.355	–	–	−0.105	−0.055	0
Uniaxial	–	–	−0.565	−0.835	−0.835	−0.205	−0.105	0
(b) $\mu_f/\mu_m = 10$ Tension	$\beta_{cM}^{(2)+}$	$\beta_{cM}^{(1)+}$	$\beta_{cM}^{(0)+}$	β_c^+	β_{cM}^+	$\beta_{cM}^{(-1)+}$	$\beta_{cM}^{(-2)+}$	$\beta_{cM}^{(R)+}$
Equibiaxial	0.055	0.105	–	–	–	–	–	0.105
Uniaxial	0.105	0.215	–	–	–	–	–	0.215
Compression	$\beta_{cM}^{(2)-}$	$\beta_{cM}^{(1)-}$	$\beta_{cM}^{(0)-}$	β_c^-	β_{cM}^-	$\beta_{cM}^{(-1)-}$	$\beta_{cM}^{(-2)-}$	$\beta_{cM}^{(R)-}$
Equibiaxial	–	–	−0.545	−0.545	−0.545	−0.105	−0.055	0
Uniaxial	–	–	−0.695	−0.485	−0.485	−0.205	−0.105	0
(c) $\mu_f/\mu_m = 50$ Tension	$\beta_{cM}^{(2)+}$	$\beta_{cM}^{(1)+}$	$\beta_{cM}^{(0)+}$	β_c^+	β_{cM}^+	$\beta_{cM}^{(-1)+}$	$\beta_{cM}^{(-2)+}$	$\beta_{cM}^{(R)+}$
Equibiaxial	0.055	0.105	–	–	–	–	–	0.105
Uniaxial	0.105	0.215	–	–	–	–	–	0.215
Compression	$\beta_{cM}^{(2)-}$	$\beta_{cM}^{(1)-}$	$\beta_{cM}^{(0)-}$	β_c^-	β_{cM}^-	$\beta_{cM}^{(-1)-}$	$\beta_{cM}^{(-2)-}$	$\beta_{cM}^{(R)-}$
Equibiaxial	–	−0.585	−0.485	−0.485	−0.485	−0.105	−0.055	0
Uniaxial	–	–	−0.535	−0.425	−0.425	−0.205	−0.105	0

The stability analysis carried out for $\mu_f/\mu_m = 50$ presents the same main features of the $\mu_f/\mu_m = 10$ case, as shown in Figs. 13 and 14. As a matter of fact, although the numerical values of the critical parameters may slightly change (see Table 3b and c), the sequence of microscopic and macroscopic primary instabilities remains unchanged. Specifically, in compression the onset of microscopic instability occurs at $\beta_c^- = -0.475$ in the equibiaxial case and at $\beta_c^- = -0.415$ in the uniaxial one. This points out that in the tiffer case the microscopic stability region in compression decreases.

For both $\mu_f/\mu_m = 10$ and $\mu_f/\mu_m = 50$, in compression, the sequence of eventual instabilities related to the conjugated stability measures remains the same of the cellular case and the loss of conditions $\overline{\mathcal{A}}^{(-1)}$ and $\overline{\mathcal{A}}^{(-2)}$ occur before the macroscopic loss of strong ellipticity. As for the cellular microstructure, in the equibiaxial compression case the loss of stability relative to the $\overline{\mathcal{A}}^{(0)}$ condition coincides with the macroscopic loss of strong ellipticity. In the uniaxial case the $\overline{\mathcal{A}}^{(0)}$ condition is eventually violated after the macroscopic loss of ellipticity both in tension and in compression.

All the above results evidence that the conditions $\overline{\mathcal{A}}^{(-1)}$ and $\overline{\mathcal{A}}^{(-2)}$ give conservative predictions in compression. It is worth noting that in the examined range of strains, in tension the conditions $\overline{\mathcal{A}}^{(-1)}$, $\overline{\mathcal{A}}^{(-2)}$ and $\overline{\mathcal{A}}^{(0)}$ always predict stability. The same consideration applies for the $\overline{\mathcal{A}}^{(2)}$ condition in equibiaxial compression.

Among the proposed conjugated stability measures, the $\overline{\mathcal{A}}^{(-1)}$ condition gives the less conservative prediction of the microscopic critical load parameter in compression. The macroscopic stability measure (28) shows the same behavior of the cellular case.

In the case of the reinforced microstructure with a neo-Hookean material the stability behavior is similar to the Gent material, with the same sequences of microscopic and macroscopic instabilities. Therefore, in the sake of brevity, for this material only the critical values of the load parameters are shown in Table 4.

Consequently, conservative stability predictions can be obtained by using $\overline{\mathcal{A}}^{(-1)}$ and $\overline{\mathcal{A}}^{(-2)}$ in compression. In addition, when the inclusion is softer than the matrix also $\overline{\mathcal{A}}^{(0)}$ is able to provide a conservative prediction.

Finally, it is worth noting that the effect of an inclusion, as expected, provides a stabilizing influence with respect to the cellular case. This stabilizing effect decreases as the inclusion becomes stiffer.

5. Conclusions and discussion

In this work, the problem of the prediction of failure mechanisms induced by microstructural instability phenomena in finitely strained composite materials with heterogeneous periodic microstructure is studied, by examining a macroscopic model of the composite developed in the framework of homogenization methodology.

The above mentioned problem is of notable relevance since an accurate direct stability analysis of the composite solid, taking into account all microstructural details, may involve a computational effort so large as to generally make this approach unviable, owing to the complexity of microstructural configuration and finite changes in constitutive and geometric microstructural properties occurring under finite strains.

Unfortunately, existing criteria based on the homogenized constitutive properties may be not able to provide a conservative prediction of microscopic instability mechanisms. As a matter of fact, the fundamental macroscopic condition introduced in the literature, corresponding to the strong ellipticity of the homogenized tangent moduli tensor, is able to provide an exact estimate of the primary microscopic instability critical load only when the instability mode has a global character (this circumstance occurs, for instance, in composite materials reinforced with relatively thick continuous fibers loaded prevalently in compression). On the contrary, the criterion based on the strong ellipticity of the homogenized moduli gives an unconservative estimation in the more general case when the instability mode is local in nature. The latter kind of instabilities may occur, for instance, in cellular solids and in composite materials reinforced with relatively thin fibers.

To this end a stability investigation on the micro- and macroscales is here developed with reference to incrementally linear materials. Novel macroscopic constitutive stability measures, based on the positive definiteness of homogenized moduli tensor associated with a class of work conjugate stress–strain measures,

are introduced and their capability to give a conservative prediction of the primary instability load of the microstructure is for the first time investigated here.

In view to computational applications, an innovative non-linear finite element procedure is developed able to solve sequentially the unit cell principal equilibrium problem, the incremental equilibrium problems giving the homogenized tangent moduli and the stability eigenvalue problem along a given monotonic macrostrain path.

The proposed approach is applied to some representative microstructures with hyperelastic constituents adopting compressible strain energy functions corresponding to Gent or neo-Hookean models. Two kinds of microgeometries are considered: a composite solid with a square arrangement of circular inclusions and a cellular material with a square distribution of circular voids. Numerical stability analyses are carried out with reference to both uniaxial and equibiaxial macrostrain loading paths.

Numerical examples highlight that the presence of a circular inclusion, although when softer than the matrix material, provides a stabilizing effect in comparison with the case of the cellular material. Moreover, the main differences in stability analyses for the two analyzed constitutive laws, are exhibited in tension especially for high levels of macrostrain.

The main result of this work is that while the critical load levels at the onset of microscopic and macroscopic instability are influenced by both the kind of microstructure (which in turn depends on the constitutive law of the constituents and on the microgeometry configuration) and the type of macroscopic loading path, their sequence depends only on the tensile or compressive nature of the macroscopic loading path, when special macroscopic stability measures are considered. Consequently, a conservative prediction of the primary microstructural instability load can be obtained by using an appropriate macroscopic stability criterion.

Specifically, results show that in the tensile case a conservative prediction of the microscopic instability load can be obtained by using the positiveness condition for the homogenized moduli tensor related to the Lagrange strain measure, $\overline{\Lambda}^{(2)}$, namely $\beta_{cM}^{(2)+} < \beta_c^+$. The same conclusion can be done with reference to the condition $\overline{\Lambda}^{(1)}$ associated to the Biot strain measure, i.e. $\beta_{cM}^{(1)+} < \beta_c^+$, with the only exception of the cellular material under uniaxial tension.

On the other hand, a conservative prediction in compression requires the use of stability measures based on homogenized moduli tensor whose corresponding strain measures are characterized by a negative value of the integer m characterizing the Hill's scale function (Hill, 1968), namely the conditions $\overline{\Lambda}^{(-1)}$ and that associated to the Almansi strain measure, $\overline{\Lambda}^{(-2)}$. As a matter of fact, it turns out that $\beta_c^- < \beta_{cM}^{(-1)-} < \beta_{cM}^{(-2)-}$.

Future developments of this work will be devoted to additional microgeometries, including defected composites with imperfectly bonded fibers, and loading paths, in order to assess the validity of the above conclusions for the most common types of composite materials.

Notation

The standard symbolic notation is used, where boldface letters represents vectors and tensors. Summation convention is employed and subscripts denote components on a fixed rectangular coordinate system. A dot between vectors and tensors denotes the scalar product:

$$\boldsymbol{A} \bullet \boldsymbol{B} \rightarrow A_i B_i \text{ or } A_{ij} B_{ij},$$

while the product between a tensor and a vector, two tensors or a fourth-order tensor and a second-order one, is denoted, respectively, as:

$$\boldsymbol{A}\boldsymbol{B} \rightarrow A_{ij} B_j \text{ or } A_{ij} B_{jk} \text{ or } A_{ijhk} B_{hk}.$$

The tensor product between two vectors or tensors is denoted as:

$$\boldsymbol{A} \otimes \boldsymbol{B} \rightarrow A_i B_j \text{ or } A_{ij} B_{hk}.$$

An upper index 'T' denotes a transpose $(A^T)_{ij} = A_{ji}$.

Det($\boldsymbol{A}$) denotes the determinant of the 3×3 matrix which has elements A_{ij}.

tr($\boldsymbol{A}$) denotes the trace of the tensor $\boldsymbol{A}$, A_{ii}.

$\|\boldsymbol{A}\|$ indicates the square root of tr($\boldsymbol{A}^T\boldsymbol{A}$).

A superposed dot over a symbol denotes differentiation by the time-like parameter τ and the subscript zero means evaluation at $\tau = 0$. $o(\tau^n)$ or $\boldsymbol{o}(\tau^n)$ denotes scalar or vectorial quantities, respectively, approaching zero faster than τ^n as $\tau \rightarrow 0$. $\boldsymbol{O}(\tau^n)$ denotes nth order terms in τ.

The abbreviated notation $\boldsymbol{f}(\boldsymbol{x})$ # or $-$# will be used to denote the periodic or antiperiodic properties of the field $\boldsymbol{f}(\boldsymbol{x})$, respectively.

The notations $\partial\phi/\partial\boldsymbol{F}$, $\partial^2\phi/\partial\boldsymbol{F}^2$ denote a second-order or a fourth-tensor whose Cartesian components are defined by $(\partial\phi/\partial\boldsymbol{F})_{ij} = \partial\phi/\partial F_{ij}$ and $(\partial^2\phi/\partial\boldsymbol{F}^2)_{ijhk} = \partial^2\phi/\partial F_{ij}\partial F_{hk}$, respectively.

References

Abeyaratne, R., Triantafyllidis, N., 1984]. An investigation of localization in a porous elastic material using homogenization theory. J. Appl. Mech. 51, 481–486.

Ball, J.M., 1977]. Convexity conditions and existence theorems in nonlinear elasticity. Arch. Ration. Mech. Anal. 63, 337–403.

Benssousan, A., Lions, J.L., Papanicoulau, G., 1978]. Asymptotic Analysis for Periodic Structures. North-Holland, Amsterdam.

COMSOL AB. COMSOL 3.4. Multiphysics user's guide, October 2007.

Cricri, G., Luciano, R., 2003]. Micro- and macro-failure models of heterogeneous media with micro-structure. Simulat. Model. Pract. Theory 11, 433–448.

De Giorgi, E., 1979. Convergence problems for functions and operators. In: De Giorgi, E. et al. (Eds.), Proceedings of the International Meeting: Recent Methods in Nonlinear Analysis, Pitagora, Bologna, Rome, pp. 131–188.

Drapier, S., Grandidier, J.C., Potier-Ferry, M., 2001]. A structural approach of plastic microbuckling in long fibre composites: comparison with theoretical and experimental results. Int. J. Solids Struct. 38, 3877–3904.

Gent, A.N., 1996]. A new constitutive relation for rubber. Rubb. Chem. Technol. 69, 59–61.

Geymonat, G., Müller, S., Triantafyllidis, N., 1993]. Homogenization of nonlinearly elastic materials, microscopic bifurcation and macroscopic loss of rank-one convexity. Arch. Ration. Mech. Anal. 122, 231–290.

Grandidier, J.C., Ferron, G., Potier-Ferry, M., 1992]. Microbuckling and strength in long-fiber composites – theory and experiments. Int. J. Solids Struct. 29, 1753–1761.

Greco, F., 2007]. An investigation on static and dynamic criteria of constitutive stability. Mech. Adv. Mater. Struct. 14 (5), 347–363 (Corrigendum: Mech. Adv. Mater. Struct. 15 (1), 77–78).

Greco, F., Luciano, R., 2005]. Analysis of the influence of incremental material response on the structural stability. Mech. Adv. Mater. Struct. 12 (5), 363–377.

Hashin, Z., Shtrikman, S., 1962]. On some variational principles in anisotropic and nonhomogeneous elasticity. J. Mech. Phys. Solids 10, 335–342.

Hassani, B., Hinton, E., 1998]. A review of homogenization and topology optimization: I. Homogenization theory for media with periodic structure. Comput. Struct. 69, 707–717.

Hill, R., 1957]. On uniqueness and stability in the theory of finite elastic strains. J. Mech. Phys. Solids 5, 229–241.

Hill, R., 1965]. A self-consistent mechanics of composite materials. J. Mech. Phys. Solids 13, 213–222.

Hill, R., 1968]. On constitutive inequalities for simple materials – I, II. J. Mech. Phys. Solids 16, 229–242.

Hill, R., 1972]. On constitutive macro-variables for heterogeneous solids at finite strain. Proc. R. Soc. Lond. A 326, 131–147.

Hill, R., 1978]. Aspects of invariance in solid mechanics. Advances in Applied Mechanics, vol. 18. Academic Press, pp. 1–72.

Hsu, S.-Y., Vogler, T.J., Kyriakides, S., 1998]. Compressive strength predictions for fiber composites. J. Appl. Mech. 65, 7–16.

Kyriakides, S., Arseculeratne, R., Perry, E.J., Liechti, E.J., 1995]. On the compressive failure of fiber-reinforced composites. Int. J. Solids Struct. 32, 689–738.

Lee, S.H., Waas, A.M., 1999]. Compressive response and failure of fiber reinforced unidirectional composites. Int. J. Fract. 100, 275–306.

Lopez-Pamies, O., Ponte Castañeda, P., 2006a]. On the overall behavior, microstructure evolution, and macroscopic stability in reinforced rubbers at large deformations: I. Theory. J. Mech. Phys. Solids 54, 807–830.

Lopez-Pamies, O., Ponte Castañeda, P., 2006b]. On the overall behavior, microstructure evolution, and macroscopic stability in reinforced rubbers at

large deformations: II. Application to cylindrical fibers. J. Mech. Phys. Solids 54, 831–863.
Lopez-Pamies, O., Ponte Castañeda, P., 2009]. Microstructure evolution in hyperelastic laminates and implications for overall behavior and macroscopic stability. Mech. Mater. 41, 364–374.
Marcellini, P., 1978]. Periodic solutions and homogenization of nonlinear variational problems. Ann. Mat. Pura Appl. 117, 139–152.
Michel, J.C., Lopez-Pamies, O., Ponte Castañeda, P., Triantafyllidis, N., 2007]. Microscopic and macroscopic instabilities in finitely strained porous elastomers. J. Mech. Phys. Solids 55, 900–938.
Miehe, C., 2003]. Computational micro-to-macro transitions for discretized micro-structures of heterogeneous materials at finite strains based on the minimization of averaged incremental energy. Comput. Methods Appl. Mech. Eng. 192, 559–591.
Miehe, C., Schroder, J., Becker, M., 2002]. Computational homogenization analysis in finite elasticity. Material and structural instabilities on the micro- and macro-scales of periodic composites and their interaction. Comput. Methods Appl. Mech. Eng. 191, 4971–5005.
Müller, S., 1987]. Homogenization of nonconvex integral functionals and cellular elastic materials. Arch. Ration. Mech. Anal. 99, 189–212.
Nemat-Nasser, S., 1999]. Averaging theorems in finite deformation plasticity. Mech. Mater. 31, 493–523.
Nestorović', M., Triantafyllidis, N., 2004]. Onset of failure in finitely strained layered composites subjected to combined normal and shear loading. J. Mech. Phys. Solids 52, 941–974.
Nezamabadi, S., Yvonnet, J., Zahrouni, H., Potier-Ferry, M., 2009]. A multilevel computational strategy for handling microscopic and macroscopic instabilities. Comput. Methods Appl. Mech. Eng. 198, 2099–2110.
Ogden, R.W., 1984]. Non-Linear Elastic Deformations. Ellis Horwood Ltd./John Wiley and Sons, Chichester, UK.
Ohno, N., Okumura, D., Noguchi, H., 2002]. Microscopic symmetric bifurcation condition of cellular solids based on a homogenization theory of finite deformation. J. Mech. Phys. Solids 50, 1125–1153.
Ponte Castañeda, P., Tiberio, E., 2000]. A second-order homogenization method in finite elasticity and applications to black-filled elastomers. J. Mech. Phys. Solids 48, 1389–1411.
Sanchez-Palencia, E., 1980]. Non-homogeneous media and vibration theory. Lecture Notes in Physics, vol. 127. Springer, Berlin, Heidelberg, New York.
Triantafyllidis, N., Bardenhagen, S.G., 1996]. The influence of scale size on the stability of periodic solids and the role of associated higher order gradient continuum models. J. Mech. Phys. Solids 44, 1891–1928.
Triantafyllidis, N., Maker, B.N., 1985]. On the comparison between microscopic and macroscopic instability mechanisms in a class of fiber-reinforced composites. ASME J. Appl. Mech. 52, 794–800.
Triantafyllidis, N., Nestorović, M.D., Schraad, M.W., 2006]. Failure surfaces for finitely strained two-phase periodic solids under general in-plane loading. J. Appl. Mech. 73, 505–515.
Vogler, T.J., Hsu, S.-Y., Kyriakides, S., 2000]. Composite failure under combined compression and shear. Int. J. Solids Struct. 37, 1765–1791.